



UvA-DARE (Digital Academic Repository)

Ferrocene-based light-responsive carbon nano hoops

Kręcijasz, R.B.

Publication date
2026

[Link to publication](#)

Citation for published version (APA):

Kręcijasz, R. B. (2026). *Ferrocene-based light-responsive carbon nano hoops*. [Thesis, fully internal, Universiteit van Amsterdam].

General rights

It is not permitted to download or to forward/distribute the text or part of it without the consent of the author(s) and/or copyright holder(s), other than for strictly personal, individual use, unless the work is under an open content license (like Creative Commons).

Disclaimer/Complaints regulations

If you believe that digital publication of certain material infringes any of your rights or (privacy) interests, please let the Library know, stating your reasons. In case of a legitimate complaint, the Library will make the material inaccessible and/or remove it from the website. Please Ask the Library: <https://uba.uva.nl/en/contact>, or a letter to: Library of the University of Amsterdam, Secretariat, P.O. Box 19185, 1000 GD Amsterdam, The Netherlands. You will be contacted as soon as possible.

2

Exploring Silyl Protecting Groups for the Synthesis of Carbon Nanohoops

Abstract

Synthesis of topological molecular nanocarbons, such as hoop-like $[n]$ cycloparaphenylenes, requires the use of spatially prearranged, masked aromatic units to overcome a build-up of large molecular strain in their curved structures. The used cyclohexadienyl units, however, contain tertiary alcohols that need protection to prevent side-reactions until the aromatization step that affords the final curved hydrocarbon. Although alkyl and triethylsilyl groups have been successfully applied as the protecting groups for this purpose, each suffers from specific drawbacks. Here, we explore the potential of sterically more crowded silyl groups, namely, *tert*-butyldimethylsilyl and triisopropylsilyl, to be used as alternatives to the established protection strategies. We show that *tert*-butyldimethylsilyl can be easily installed and deprotected under mild conditions displaying markedly higher resistance towards acids or bases than the triethylsilyl group used to this date. Unlike in the case of the alkyl groups, *tert*-butyldimethylsilyl also preserves a high stereoselectivity of the nucleophilic additions of ArLi. Furthermore, we demonstrate that both *tert*-butyldimethylsilyl and triethylsilyl groups can be installed on the same substrate and the latter be selectively deprotected. Thus, the high stereoselectivity, improved stability, and easy deprotection make *tert*-butyldimethylsilyl an excellent protecting group for the synthesis of carbon nanohoops.

The content of this chapter has been published as: **R. B. Křečijasz**, J. Malinčík, T. Šolomek. Exploring Silyl Protecting Groups for the Synthesis of Carbon Nanohoops. *Synthesis* **2023**, *55*, 1355–1366.

2.1 Introduction

Protecting groups are an indispensable tool to control selectivity of chemical transformations in modern natural product synthesis or synthesis of organic materials. An ideal protecting group needs to match several criteria, such as high-yielding introduction and removal steps, sufficient stability and highly specific deprotection conditions to afford orthogonality towards other protecting groups. A particularly useful type of scaffolds bearing tertiary alcohols, which require protection are **A** and **B** (Figure 2.1). For example, compounds **1** and **2** (Figure 2.2) that contain scaffolds **A** and **B**, are important building blocks in the synthesis of topological molecular nanocarbons that involve carbon nano hoops, such as $[n]$ cycloparaphenylenes ($[n]$ CPPs).^[1–12] Carbon nano hoops exhibit unique size-dependent optoelectronic properties^[13–17] and host-guest chemistry^[18–27] giving rise to applications in bioimaging, optoelectronic materials and supramolecular carbon-rich nanomaterials.^[28–37] Although envisioned decades ago, the first synthesis of these strained molecules was accomplished only in 2008 by Jasti and Bertozzi.^[38] Their strategy relies on masking a *p*-phenylene unit as a 1,4-dimethoxycyclohexa-2,5-diene-1,4-diyl moiety. Here, the two tertiary alcohols prearrange the geometry in scaffold **B** with *cis* configuration for an effective macrocyclization. The reductive aromatization of the cyclohexa-2,5-diene unit then provides the necessary driving force to build up the strain in the final step.

The exergonicity of the aromatization, however, requires that the tertiary alcohols be protected throughout the multistep synthesis to avoid side-reactions. The electronic nature and the size of the methyl group used originally, however, result in a poor diastereoselectivity of the addition of organolithium reagents, typically ArLi, to ketone scaffold **A**.^[38,39] Moreover, their removal during the aromatization often necessitates the use of harsh reagents, such as lithium/sodium

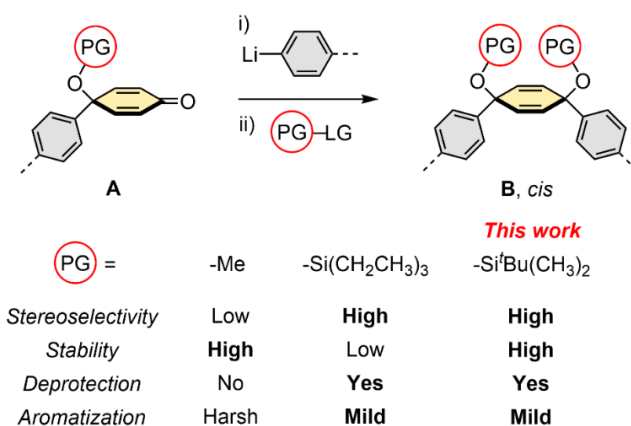


Figure 2.1. Protection of important structural scaffolds **A** and **B** in the synthesis of carbon nano hoops.

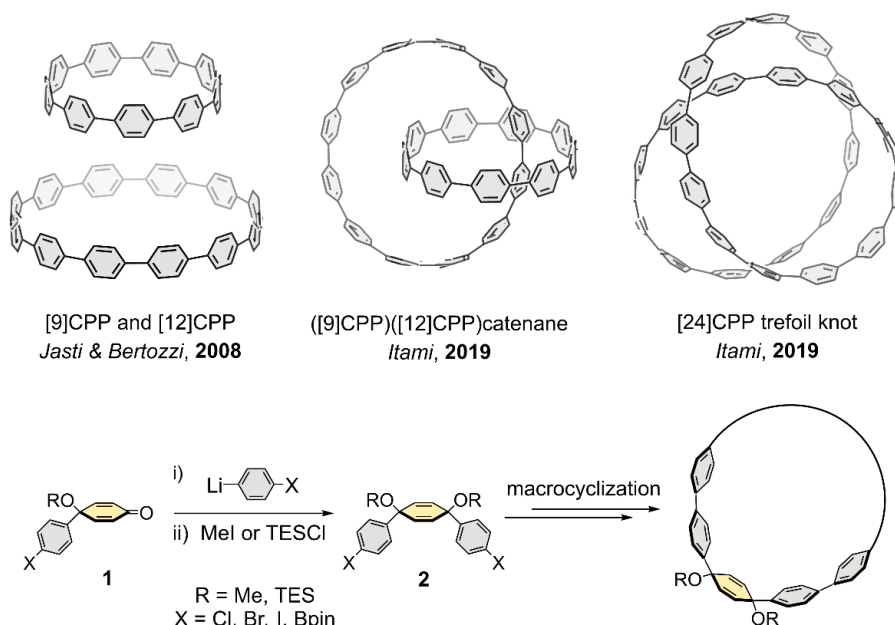


Figure 2.2. Topological molecular nanocarbons based on cycloparaphenylene nanohoops (top) and their synthesis using scaffolds **A** and **B** (bottom).^[9,38]

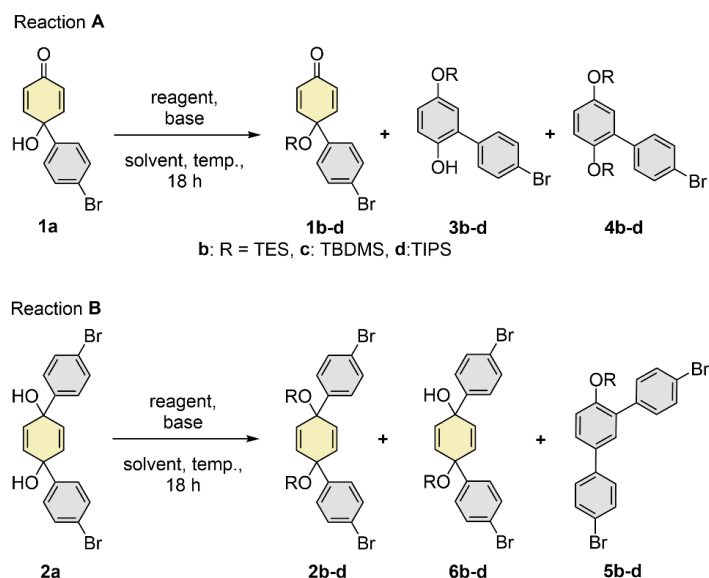
naphthalide. Although the diastereoselectivity of the addition was found to be mostly dictated by electrostatics,^[40,41] Yamago and co-workers^[42,43] proposed the use of bulkier triethylsilyl (TES) as the protecting group for the tertiary alcohols in **A** or **B**. TES improves the stereoselectivity of ArLi addition and the exclusive formation of the *cis*-diastereomer of **B** is typically observed. TES is also relatively straightforward to deprotect with tetra-*n*-butylammonium fluoride (TBAF) before the aromatization of the ensuing 1,4-dihydroxycyclohexa-2,5-diene-1,4-diyl, performed under mild conditions with H_2SnCl_4 .^[41] In our own experience, however, the sensitivity of the TES group towards acids compromises the stability of compounds that contain the structural motif **B**. Such compounds are prone to decomposition either during the purification step after their synthesis or when stored even at low temperatures, although such negative results are rarely reported in the literature.^[11,31,44,45] Because of the individual drawbacks of the methyl and TES groups, we decided to search for an alternative protecting group that would (a) be easy to introduce, (b) undergo stereoselective addition of the ArLi to ketones **A**, (c) be significantly more stable than TES and (d) easy to remove to allow for a mild aromatization. Such protecting group could introduce additional orthogonality to the synthesis of topological molecular nanocarbons.

The steric bulk around the silicon determines the stability of a silyl protecting group permitting a selective protection/deprotection in the presence of another silyl ether.^[46–51] The stability of TES ethers used in **A** and **B** is relatively low in comparison to other silyl ethers in the presence of both

acids and bases. For example, the half-lives of TES protected *p*-cresol in the presence of 1% hydrochloric acid or 5% sodium hydroxide are <1 minute, while the half-lives of *tert*-butyldimethylsilyl (TBDMS) protected *p*-cresol are 273 minutes and 3.5 minutes, respectively.^[50] In general, the relative stability of different silyl groups to acids increase in the following order: trimethylsilyl (TMS; 1) < TES (64) < TBDMS (20,000) < triisopropylsilyl (TIPS; 700,000) < *tert*-butyldiphenylsilyl (TBDPS; 5,000,000), while to bases the order is: TMS (1) < TES (10–100) < TBDMS ~ TBDPS (20,000) < TIPS (100,000).^[51] Therefore, protecting groups with additional steric bulk, such as TBDMS or TIPS, represent great candidates for a considerably more stable protecting group. In addition, the extra steric bulk of a silyl ether in **A** is expected to display excellent diastereoselectivity of an ArLi nucleophilic addition to form the motif **B**. Protection of a tertiary alcohol, however, becomes more challenging with the increasing steric bulk of the silyl protecting group.^[52] As a result, we expected to initially face some obstacles to install two such sterically demanding groups in a close proximity in **B**.

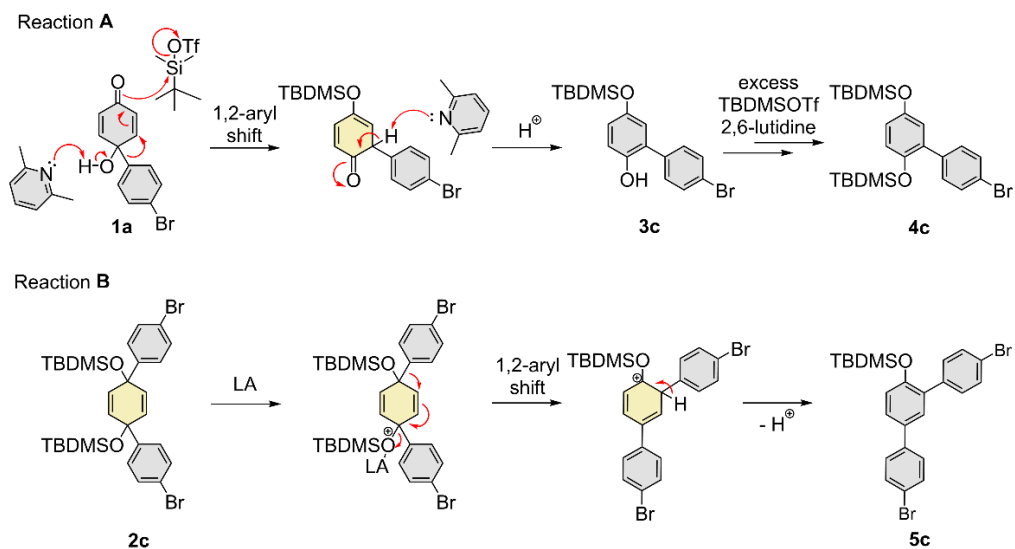
2.2 Results and Discussion

We selected model alcohols **1a** and **2a** (Scheme 2.1) as proxies for the motifs **A** and **B**, respectively. In fact, these two alcohols are frequently used in the synthesis of carbon nanohoops including CPPs^[1–12,38,39,41,42,53–66] and their protection with TES to **1b** and **2b** can be achieved in



Scheme 2.1. Introduction of silyl protecting groups to scaffolds **A** and **B** using two model alcohols **1a** and **2a**.

92%^[6] and $\geq 82\%$ ^[41] yield, respectively, in a clean transformation. We first tested the standard silylation of **1a** with *tert*-butyldimethylsilyl chloride (TBDMSCl) and imidazole^[67] in CH₂Cl₂ at room temperature (Table 2.1, entry 1; Table S2.1, entry 1) and obtained a full conversion of **1a**. However, we observed formation of a complicated mixture of unknown products. We assumed that the steric bulk slows down the nucleophilic substitution of the chloride in TBDMSCl allowing other reactions to compete. We changed CH₂Cl₂ for significantly more polar DMF, which we expected to stabilize the alcoholate that could be generated from **1a** and imidazole in a very small amount. Such attempts resulted only in a slow conversion of **1a** to an unknown product, even when larger amounts of the reagents and elevated temperature were used (Table 2.1, entry 2). Diol **2a** was completely inert under the same reaction conditions (Table 2.1, entry 5). Similarly, **1a** turned unreactive when the bulkier 2,6-lutidine with a similar basicity was used (Table 2.1, entry 3). Likely, the observed side-reactions are catalyzed by a general base. To accelerate the nucleophilic substitution at silicon, we decided to replace the chloride in TBDMSCl for triflate, which is an excellent nucleofuge. The combination of 2,6-lutidine with *tert*-butyldimethylsilyl trifluoromethanesulfonate (TBDMSOTf) in CH₂Cl₂, however, afforded a full conversion of **1a** to **3c** and **4c** (Table S2.1, entry 4). Product **3c** is most probably formed through a rearrangement involving a 1,2-aryl shift (Scheme 2.2), while **4c** ensues from the excess TBDMSOTf reacting with **3c**. The observed transformation nicely illustrates the power of aromatization to drive rearrangements of cyclohexadienones.^[68–72] To our satisfaction, we observed the formation of **1c** when the reaction was repeated under the same conditions but in polar DMF, albeit the reaction



Scheme 2.2. Proposed mechanisms for the observed rearrangements of **1a** and **2c**. LA = Lewis acid.

Table 2.1. Optimization of reaction conditions to introduce silyl ethers to **1a** and **2a**.

Entry	Reagent (equiv.)	Base (equiv.)	Solvent	Temp. (°C)	Ratio ^a	Yield ^b (%)
		1a:1c:3c:4c		1c	3c	4c
Reaction A						
1	TBDMSCl (2)	Imidazole (3)	CH ₂ Cl ₂	RT ^c	0:0:0:0 ^d	-
2	TBDMSCl (5)	Imidazole (6)	DMF	60	<100:0:0:0 ^{e,d}	-
3	TBDMSCl (5)	2,6-lutidine (6)	DMF	70	n.c. ^f	-
4	TBDMSTf (2.5)	2,6-lutidine (4)	DMF	70	0:82:0:18	63 (71) ^g
Reaction B						
		2a:2c:6c:5c		2c	6c	5c
5	TBDMSCl (5)	Imidazole (6)	CH ₂ Cl ₂	RT	n.c.	-
	TBDMSCl (5)	Imidazole (6)	DMF	70	n.c.	-
6	TBDMSTf (5)	2,6-lutidine (6)	DMF	70	0:52:0:48	-
7	TBDMSTf (5)	2,6-lutidine (6)	DMF	50	0:98:0:2	70
Reaction A						
		1a:2d:3d:4d		1d	3d	4d
8	TIPSOTf (5)	2,6-lutidine (6)	DMF	70	- ^j	3
Reaction B						
		2a:2d:6d:5d		2d	6d	5d
9	TIPSOTf (5)	2,6-lutidine (6)	DMF	50	46:0:49:5	0
					39	6 ^k

^a Ratio of products determined by ¹H NMR in CDCl₃ after 18 h. ^b Yield of the isolated product after 18 h. ^c RT = room temperature. ^d Formation of unidentified product(s). ^e Products ratio determined after 38 h. ^f n.c. = no conversion. ^g Performed on 1.00 g (3.77 mmol) scale. ^h Compound **5c** was isolated along with a minor unidentified product. ⁱ Determination of the ratio was not successful due to overlap of the ¹H resonances. ^j Compound **1a** was recovered in 36% yield. ^k Compound **2a** was recovered in 35% yield.

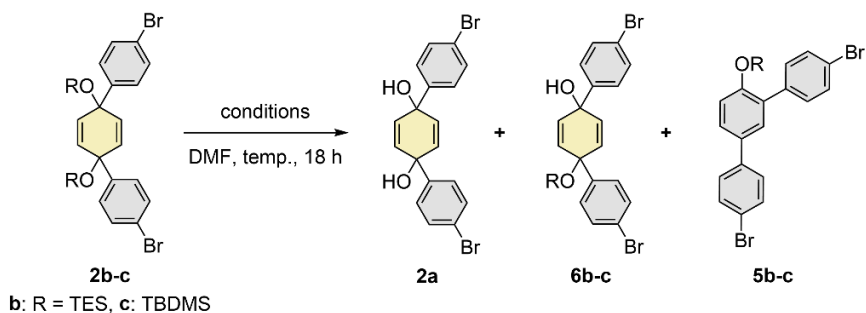
appeared slower (Table S2.1, entry 5). Increasing the amounts of the TBDMSOTf and 2,6-lutidine and increasing the temperature provided a faster reaction, which was, however, accompanied by the formation of **4c** (Table S2.1, entries 6–10). The optimal temperature was found to be 70 °C because it resulted in a full conversion of **1a** in 18 hours (incomplete at 60 °C) and a lower yield of **4c** compared to the reaction at 80 °C. The reaction at 70 °C afforded **1c** and **4c** in 58% and 8% isolated yields, respectively, after an easy separation by column chromatography. Finally, the reduction of the amounts of the reagents and solvent (Table S2.1, entries 11–17) provided the optimal conditions that allowed us to isolate **1c** in 71% yield on one gram scale (Table 2.1, entry 4). We also tested different bases in combination with TBDMSOTf (Table S2.1, entries 18–23) but the reaction was slower or no significant improvement of the **1c:4c** ratio or the isolated yield of **1c** could be achieved.

We next attempted the protection of diol **2a** with TBDMSOTf (Scheme 2.1, Reaction **B**). The optimal conditions found for the protection of **1a** led to a full conversion of **2a** (Table 2.1, entry 6). In addition to the desired product **2c**, however, formation of a significant portion of **5c** was observed. Similar to the formation of **3c**, this rearrangement involves a 1,2-aryl shift aromatizing the cyclohexa-2,5-diene-1,4-diyl unit (Scheme 2.2). Increasing the amount of TBDMSOTf and 2,6-lutidine improved the relative yield of **2c** (Table S2.2, entry 3). In analogy to our experiments with **1a**, we hypothesized that the rate-limiting step in the rearrangement has a higher barrier. We noticed almost exclusive formation of **5c** at 100 °C, while the reaction at 40 °C showed the opposite effect and provided mostly **2c** (Table S2.2, entries 4–5). At room temperature, however, a small amount of the monoprotected **6c** was observed (Table S2.2, entry 6). Finally, the reaction performed at 50 °C with a reduced amount of TBDMSOTf and 2,6-lutidine provided the best result (Table 2.1, entry 7). Compounds **2c** and **5c** are relatively nonpolar with similar retention factors. Nevertheless, we achieved their full separation by column chromatography and isolated **2c** in 70 % yield. Although the isolated yields upon protection with TBDMS are somewhat lower than those with TES, the optimized protocols provide satisfactory results that improve with the reaction scale and allow for using TBDMS protection in a multistep synthesis of hoop-like molecular nanocarbons.

We were then interested whether the steric bulk on silicon could further be increased. We thus attempted protecting **1a** with TIPSOTf and the base and solvent used in the case of TBDMSOTf (Table 2.1, entry 4). We reached an incomplete conversion after 18 hours isolating the desired TIPS-protected **1d** in only 3% yield along with the rearranged product **4d** in 34% yield (Table 2.1, entry 8). Similar unsatisfactory result was obtained when **2a** was reacted with TIPSOTf (Table 2.1, entry 9). In this case, no formation of the doubly protected **2d** was observed. Instead, the reaction afforded the monoprotected product **6d** in 39% isolated yield together with 6% of the

rearranged product **5d**. Although increasing the amounts of TIPSOTf and base and elevating the temperature allowed to improve the conversion (Table S2.3, entries 3–4), heating favored the formation of **5d**, the exclusive product at 100 °C. Clearly, the bulkiness of the TIPS group leads to its relatively difficult introduction to **1a** and precludes installing two TIPS protecting groups to **2a** due to their proximity in **2d**.

The nearly exclusive formation of **5c** at 100 °C (Table S2.2, entry 4) was rather intriguing because we expected the formation of **2c** and **5c** in similar portions if the protection and the rearrangement were parallel processes. The result, instead, suggests that it is the **2c** that is transformed into **5c** in a subsequent reaction. We thus conducted a series of experiments to determine conditions that promote the rearrangement and that may have a detrimental effect on the stability of **2c**. When a DMF solution of **2c** was stirred at 100 °C with or without addition of 2,6-lutidine, no conversion of **2c** was observed (Table 2.2, entries 1–2). Excess of TBDMSOTf in the absence of base converted **2c** fully into **5c**, which we isolated in 83% yield (Table 2.2, entry 3). Using excess of TBDMSCl, a weaker Lewis acid, did not show any sign of rearrangement (Table 2.2, entry 4). It indicates that TBDMSOTf may act in the rearrangement as a Lewis acid.^[44,45] We suspected that TBDMSOTf may contain traces of triflic acid (TfOH) that could catalyze the rearrangement. Indeed, a catalytic amount (10 mol%, Table 2.2, entry 5) of TfOH led to a clean rearrangement of **2c** at 100 °C furnishing **5c**, which we isolated in 84% yield. It is worth noting that the second TBDMS group in **5c** was not cleaved during the reaction. The TBDMS group is known to be more resistant to acidic conditions than the TES group^[51] which motivated us to compare their stability in **2b** and **2c** in the presence of acids, such as TFA, HCl, and TfOH. In a typical experiment, a DMF solution of **2b** or **2c** was stirred with a catalytic amount of the selected acid at 35 °C for 18 hours and the reaction progress was monitored by ¹H NMR spectroscopy (Table 2.2, entries 6–9). Compound **2c** was inert to the presence of TFA ($pK_a = 0.52$ in water^[73]), while a partial deprotection of one of the TES groups in **2b** was observed. A much stronger HCl ($pK_a = -5.9$ ^[74]) affected neither **2b** nor **2c** when only 1 mol% of the acid was used. Increasing the amount of HCl to 10 mol%, however, promoted the deprotection of the TES groups, while the TBDMS was inert. No rearrangement was observed in any of these attempts. Both **2b** and **2c** reacted in the presence of 10 mol% of very strong TfOH ($pK_a = -14.7$ ^[74]). Only a partial conversion of **2c** was reached after 18 hours at 35 °C compared to the full rearrangement to **5c** at 100 °C (Table 2.2, entries 5 and 9) and no TBDMS deprotection could be detected. On the other hand, **2b** was fully transformed to a mixture of unknown products. These results indicate that **2c** is considerably more persistent to acids than **2b**. In our experience, some TES-protected moieties similar to **2b** (see **2** in Figure 2.2) are surprisingly labile.^[44,45] Their stability is influenced by solvent and traces of impurities. For example, we even observed a rearrangement analogous to **2c**→**5c** in the presence of Mg²⁺ ions

Table 2.2. Stability of **2b** and **2c** at different conditions.

Entry	Conditions	Substrate	Result ^a
1	No additives, 100 °C	2c	n.c. ^b
2	2,6-lutidine (12 equiv.), 100 °C	2c	n.c.
3	TBDMSOTf (10 equiv.), 100 °C	2c	2c:5c = 0:100 ^c
4	TBDMSCl (10 equiv.), 100 °C	2c	n.c.
5	TfOH (10 mol%), 100 °C	2c	2c:5c = 0:100 ^d
6	TFA (10 mol%), 35 °C ^e	2b	2b:6b = 83:17
		2c	n.c.
7	HCl (1 mol%), 35 °C	2b	n.c.
		2c	n.c.
		2c	2b:2a:6b = 63:8:29
8	HCl (10 mol%), 35 °C	2b	2b:2a:6b = 63:8:29
		2c	n.c.
9	TfOH (10 mol%), 35 °C	2b	Unknown product(s) and traces of 2a
		2c	2c:5c = 83:17

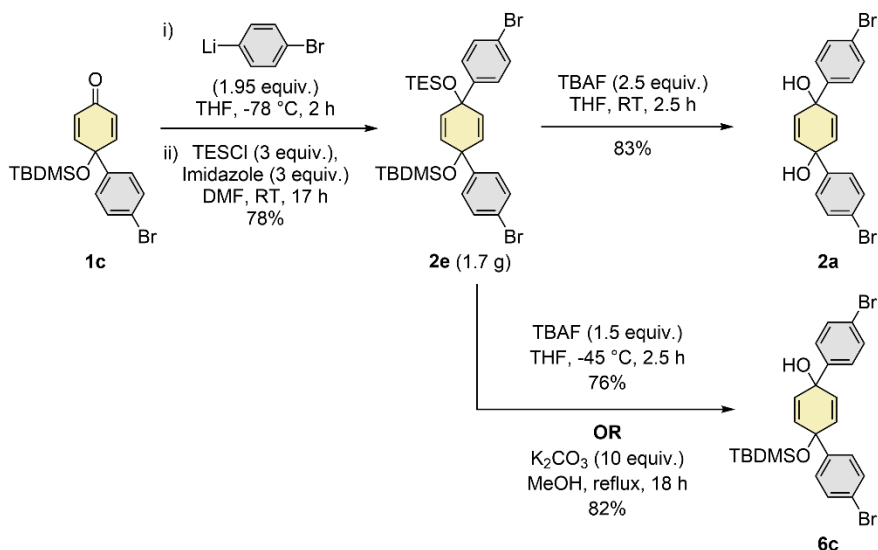
^a Ratio of products determined by ¹H NMR in CDCl₃ after 18 h. ^b n.c. = no conversion. ^c Compound **5c** isolated in 83% yield. ^d Compound **5c** isolated in 84% yield. ^e Temperature required to dissolve **2c** in DMF.

in one specific case.^[75] We thus expect that many issues with the stability of the building blocks (**1** and **2** in Figure 2.2) used in the synthesis of hoop-like molecular nanocarbons that rely on the strategy employing triethylsilyl protecting groups (TES) can now be avoided by using the TBDMS. Clearly, the 1,2-aryl shift in **2c** with TBDMS groups in DMF requires a very strong Lewis or Brønsted acid and an elevated temperature to proceed on a reasonable timescale (see Scheme 2.2 for the proposed mechanism). However, we cannot exclude that the formation of **5c** first involves a rapid formation of **6c**, although our results with HCl indicate that this process is likely not particularly facile.

We then aimed to demonstrate that TBDMS protecting group in **1c** preserves a high stereoselectivity of an ArLi addition to the carbonyl group and that both TBDMS and TES groups

could be installed on a single 1,4-dihydroxycyclohexa-2,5-diene-1,4-diyl moiety as in compound **2e** (Scheme 2.3), and the latter selectively removed in a subsequent step. The addition was accomplished with monolithiated 1,4-dibromobenzene to **1c** at $-78\text{ }^{\circ}\text{C}$ followed by the protection of the resulting alcohol with the TES group to provide 1.7 g of **2e** in 78% yield. We noticed the formation of a single *cis* diastereomer, which confirms that TBDMS displays the same high stereoselectivity as observed for **1b** bearing the TES group. We fully deprotected both silyl groups with TBAF at room temperature, isolating **2a** in 83% yield. Similarly, both TBDMS groups in **2c** could be cleaved in 73% yield. When the temperature was decreased to $-45\text{ }^{\circ}\text{C}$, we successfully achieved a selective deprotection of TES in **2e** affording **6c** in 76% yield. Similarly, a selective deprotection of TES could also be accomplished in 82% yield when **2e** was stirred with an excess of K_2CO_3 in refluxing methanol. The selective deprotection of the TES can be thus easily achieved under mild conditions with two complementary methods. As such, combination of both silyl groups represents an attractive strategy to construct versatile building blocks that may prove useful beyond the synthesis of macrocycles found in the topological molecular nanocarbons.

Finally, we evaluated the effect of the steric bulk of the protecting groups on the “bite” angle defined by the two phenylenes attached to the central cyclohexadienyl unit in **2**. Building blocks such as **2** are key intermediates in the synthesis of a variety of carbon nano-hoops and the size of the bite angle may affect the efficiency of the macrocyclization step. The steric hindrance



Scheme 2.3. Synthesis of **2e** and its selective deprotection to **2a** or **6c**.

between two bulky protecting groups, such as the TBDMS, could decrease this angle and prevent the macrocycle formation if a wider bite angle was required. Therefore, we compared the impact of the protecting group size (Me, TMS, TBDMS) in **2** on the bite angle using DFT calculations. We found out that the value of the bite angle in **2** ($65^{\circ}\pm 5^{\circ}$) is not particularly sensitive to the type of the protecting group (see Table S2.4). Analysis of the few reported^[54,76] crystal structures of compounds analogous to **2** (see Figures S2.1–S2.3, Table S2.4) to validate the accuracy of the selected DFT functionals confirmed that our calculations reproduce the bite angles well. In addition, the analysis of the crystal structures further revealed that the phenylenes can adopt surprisingly acute bite angles (47°). As a result, one can expect that **2c** with bulky TBDMS protecting groups can be used in place of **2b** (or Me-protected **2a**) in the synthesis of carbon nanohoops. However, in cases where the TES introduction or removal steps prevent successful synthesis of a carbon nanohoop, the use of TBDMS will likely lead to the same outcome.

2.3 Conclusion

In conclusion, we demonstrated that *tert*-butyldimethylsilyl is a versatile protecting group in the synthesis of important building blocks used in the synthesis of topological molecular nanocarbons, such as hoop-like CPPs. We developed the methodology to install and cleave *tert*-butyldimethylsilyl under mild conditions minimizing undesired rearrangements driven by aromatization of cyclohexa-2,5-diene-1,4-diyl units. The tested *tert*-butyldimethylsilyl ethers were substantially more stable towards acids and bases than the corresponding triethylsilyl groups frequently used to this date. The steric bulk in the *tert*-butyldimethylsilyl preserves a high stereoselectivity of ArLi additions to afford spatially prearranged building blocks used in the CPP synthesis. We also explored the conditions that trigger the undesired rearrangements involving 1,2-aryl shifts. In addition, we successfully prepared a compound with both *tert*-butyldimethyl and triethylsilyl ethers and identified conditions that permit removing the triethylsilyl chemoselectively. We anticipate that the strategies developed in this work will find applications in the synthesis of carbon nanohoops, such as CPPs and their derivatives, but also of other macrocycles, e.g., unprecedented macrocyclic drugs, that incorporate a biphenyl or a terphenyl moiety.

2.4 Appendix

Unless otherwise stated, all glassware used to perform moisture-sensitive reactions was oven-dried at 120 °C overnight, assembled hot and allowed to cool down to room temperature under a stream of argon, or flame-dried under high vacuum and filled with argon. All reactions that require heating were conducted in an oil bath and the indicated temperature corresponds to the temperature of the oil bath. To obtain a temperature of –78 °C or –45 °C, a bath of acetone or acetonitrile, respectively, was cooled with dry ice. All commercially available reagents and solvents were used directly without purification unless stated otherwise. Flash column chromatography was performed using silica gel 60 Å (230–400 mesh particle size) from Supelco®. Thin layer chromatography (TLC) was performed on silica gel plates F₂₅₄ 60 (aluminum supported) from Supelco® using UV (254 nm) visualization. ¹H and ¹³C NMR spectra were recorded on a Bruker Avance II 400 or a Bruker Avance III HD 400 spectrometer (¹H: 400 MHz, ¹³C: 101 MHz), or Bruker Avance III HD 300 (¹H: 300 MHz, ¹³C: 75 MHz). Chemical shifts (δ) were reported in parts per million (ppm) referenced to residual solvent peak (¹H: 7.26 ppm for CDCl₃, 5.32 ppm for CD₂Cl₂; ¹³C: 77.16 ppm for CDCl₃, 53.84 ppm for CD₂Cl₂). Multiplicities are given as s (singlet), d (doublet), t (triplet), q (quadruplet), m (multiplet), and br (broad). High resolution mass spectra (HRMS) were recorded on ThermoScientific LTQ Orbitrap XL mass instrument using nanoelectrospray (NSI-MS) or electron ionization (EI-MS). Elemental analysis was performed in triplicate on Thermo Scientific Flash 2000 Series instrument using CHN method with sulfanilamide or cyclohexanone as reference. Melting points were determined on Büchi B-545 apparatus and are uncorrected.

2.4.1 Experimental procedures

4'-bromo-1-hydroxy-[1,1'-biphenyl]-4(1*H*)-one (1a)

We modified a literature procedure:^[39] To a solution of 4'-bromo-(1,1'-biphenyl)-4-ol (20.00 g, 80.3 mmol, 1 equiv., CAS: 29558-77-8) and imidazole (8.75 g, 128.0 mmol, 1.6 equiv., CAS: 288-32-4) in CH₂Cl₂ (210 mL) was added chlorotrimethylsilane (14.0 mL, 128.0 mmol, 1.6 equiv., CAS: 75-77-4) at 0 °C. The reaction mixture was allowed to warm up to room temperature and stirred for 19 h. The reaction was quenched with saturated aqueous NaHCO₃ solution (60 mL) and extracted with CH₂Cl₂ (3 x 50 mL). The organic layers were combined, washed one additional time with saturated aqueous NaHCO₃ solution (100 mL) and brine (100 mL), dried over anhydrous Na₂SO₄, filtered, and concentrated in vacuo to afford a beige solid which was used in the next step without further purification.

Chapter 2

(Diacetoxyiodo)benzene (33.62 g, 104.4 mmol, 1.3 equiv., CAS: 3240-34-4) was added to a solution of the obtained solid in THF (300 mL), distilled H₂O (130 mL) and MeCN (75 mL) portionwise over 30 min. The reaction mixture was stirred at room temperature for 21.5 h. The solvents were then removed in vacuo to afford an orange solid. Crude product was purified by flash chromatography (SiO₂, EtOAc: *n*-pentane = 1:4 → EtOAc: *n*-pentane = 1:0, then MeOH: EtOAc = 1:19) to afford **1a** as a pale orange solid (17.26 g, 65.1 mmol, 81%). Spectral data match the literature-reported values.^[39]

Pale orange solid; *R_f* = 0.27 (SiO₂, EtOAc: *n*-pentane = 3:7); Mp 176–177°C.

¹H NMR (300 MHz, CDCl₃): δ = 7.51 (d, *J* = 8.7 Hz, 2H), 7.35 (d, *J* = 8.7 Hz, 2H), 6.85 (d, *J* = 10.1 Hz, 2H), 6.25 (d, *J* = 10.0 Hz, 2H), 2.39 (s, 1H).

¹³C NMR (101 MHz, CDCl₃): δ = 185.44, 150.20, 137.90, 132.20, 127.37, 127.27, 122.74, 70.88.

HRMS (NSI): *m/z* [M – H]⁺ calcd for C₁₂H₈O₂Br: 262.9713; found: 262.9706.

Anal. Calcd for C₁₂H₉O₂Br: C, 54.37; H, 3.42. Found: C, 54.52; H, 3.46.

4'-bromo-1-((triethylsilyl)oxy)-[1,1'-biphenyl]-4(1*H*)-one (**1b**)

According to known literature procedure,^[6] chlorotriethylsilane (0.475 mL, 2.83 mmol, 3 equiv., CAS: 994-30-9) was added to a solution of **1a** (500.0 mg, 1.89 mmol, 1 equiv.) and imidazole (257.0 mg, 3.77 mmol, 2 equiv.) in DMF (10 mL). The reaction mixture was stirred at 40 °C for 15 h. The reaction was quenched with saturated aqueous NaHCO₃ solution (10 mL) and extracted with EtOAc (3 x 15 mL). The organic layers were combined, washed with saturated aqueous NaHCO₃ solution (50 mL), H₂O (2 x 50 mL), brine (50 mL), dried over anhydrous Na₂SO₄, filtered and concentrated in vacuo to afford an orange oil. Crude product was purified by flash chromatography (SiO₂, EtOAc: *n*-pentane = 1:99 → EtOAc: *n*-pentane = 3:97) to afford **1b** as a yellow oil (539.8 mg, 1.42 mmol, 75%). Spectral data match the literature-reported values.^[6]

Yellow oil; *R_f* = 0.30 (SiO₂, EtOAc: *n*-pentane = 1:19).

¹H NMR (400 MHz, CDCl₃): δ = 7.46 (d, *J* = 8.6 Hz, 2H), 7.31 (d, *J* = 8.7 Hz, 2H), 6.78 (d, *J* = 10.1 Hz, 2H), 6.22 (d, *J* = 10.0 Hz, 2H), 0.97 (t, *J* = 7.9 Hz, 9H), 0.65 (q, *J* = 7.9 Hz, 6H).

¹³C NMR (101 MHz, CDCl₃): δ = 185.73, 151.62, 139.29, 131.95, 127.35, 126.89, 122.23, 72.96, 7.02, 6.35.

HRMS (NSI): *m/z* [M + H]⁺ calcd for C₁₈H₂₄O₂BrSi: 379.0723; found: 379.0721.

Anal. Calcd for C₁₈H₂₃O₂BrSi: C, 56.99; H, 6.11. Found: C, 56.89; H, 5.99.

4'-bromo-1-((*tert*-butyldimethylsilyl)oxy)-[1,1'-biphenyl]-4(1*H*)-one (1c)

To a solution of **1a** (200.0 mg, 0.754 mmol, 1 equiv.) in DMF (10 mL) 2,6-lutidine (0.351 mL, 3.02 mmol, 4 equiv., CAS: 108-48-5) was added, followed by *tert*-butyldimethylsilyl trifluoromethanesulfonate (0.433 mL, 1.89 mmol, 2.5 equiv., CAS: 69739-34-0). The reaction mixture was stirred at 70 °C for 18 h. The reaction was quenched with saturated aqueous NaHCO₃ solution (10 mL) and extracted with EtOAc (3 x 10 mL). The organic layers were combined, washed with H₂O (2 x 30 mL) and concentrated in vacuo to afford a dark orange oil. Crude product was purified by flash chromatography (SiO₂, EtOAc: *n*-pentane = 1:99 → EtOAc: *n*-pentane = 1:19) to afford **4c** as a white solid (36.8 mg, 0.075 mmol, 10%) and **1c** as a white solid (197.8 mg, 0.521 mmol, 69%).

White solid; *R*_f = 0.29 (SiO₂, EtOAc: *n*-pentane = 1:19); Mp 88–89 °C.

¹H NMR (400 MHz, CDCl₃): δ = 7.46 (d, *J* = 8.6 Hz, 2H), 7.31 (d, *J* = 8.6 Hz, 2H), 6.79 (d, *J* = 10.0 Hz, 2H), 6.23 (d, *J* = 10.1 Hz, 2H), 0.97 (s, 9H), 0.12 (s, 6H).

¹³C NMR (101 MHz, CDCl₃): δ = 185.66, 151.67, 139.34, 131.96, 127.31, 126.92, 122.23, 73.15, 25.86, 18.54, -2.49.

HRMS (NSI): *m/z* [M + H]⁺ calcd for C₁₈H₂₄O₂BrSi: 379.0723; found: 379.0707.

Anal. Calcd for C₁₈H₂₃O₂BrSi: C, 56.99; H, 6.11. Found: C, 57.10; H, 6.18.

4'-bromo-5-((*tert*-butyldimethylsilyl)oxy)-[1,1'-biphenyl]-2-ol (3c)

To a solution of **1a** (200.0 mg, 0.754 mmol, 1 equiv.) in CH₂Cl₂ (10 mL) 2,6-lutidine (0.263 mL, 2.26 mmol, 3 equiv.) was added, followed by *tert*-butyldimethylsilyl trifluoromethanesulfonate (0.346 mL, 1.51 mmol, 2 equiv.). The reaction mixture was stirred at room temperature for 18 h. The reaction was quenched with saturated aqueous NaHCO₃ solution (10 mL) and extracted with CH₂Cl₂ (3 x 10 mL). The organic layers were combined, washed with brine (50 mL), dried over anhydrous Na₂SO₄, filtered and concentrated in vacuo to afford an orange solid. Crude product was purified by flash chromatography (SiO₂, EtOAc: *n*-pentane = 1:19) to afford **4c** as a white solid (194.7 mg, 0.392 mmol, 52%) and **3c** as a pale orange solid (49.3 mg, 0.130 mmol, 17%).

Pale orange solid; *R*_f = 0.32 (SiO₂, EtOAc: *n*-pentane = 1:9); Mp 77–78 °C.

Chapter 2

^1H NMR (400 MHz, CDCl_3): 7.60 (d, $J = 8.4$ Hz, 2H), 7.35 (d, $J = 8.4$ Hz, 2H), 6.81 (d, $J = 8.5$ Hz, 1H), 6.74 (dd, $J = 8.5, 2.9$ Hz, 1H), 6.71 (d, $J = 2.9$ Hz, 1H), 4.74 (s, 1H), 0.99 (s, 9H), 0.19 (s, 6H).

^{13}C NMR (101 MHz, CDCl_3): $\delta = 149.58, 146.71, 136.34, 132.29, 130.89, 127.74, 122.08, 121.35, 120.76, 116.88, 25.85, 18.32, -4.31$.

HRMS (NSI): m/z $[\text{M} + \text{H}]^+$ calcd for $\text{C}_{18}\text{H}_{24}\text{O}_2\text{BrSi}$: 379.0723; found: 379.0721.

Anal. Calcd for $\text{C}_{18}\text{H}_{23}\text{O}_2\text{BrSi}$: C, 56.99; H, 6.11. Found: C, 57.06; H, 6.16.

((4'-bromo-[1,1'-biphenyl]-2,5-diyl)bis(oxy))bis(tert-butyl dimethylsilane) (4c)

See compound **1c** or **3c** for the procedure.

White solid; $R_f = 0.69$ (SiO_2 , EtOAc: *n*-pentane = 1:99); Mp 78–79 °C.

^1H NMR (300 MHz, CDCl_3): $\delta = 7.49$ (d, $J = 8.5$ Hz, 2H), 7.36 (d, $J = 8.5$ Hz, 2H), 6.76 (d, $J = 8.7$, 1H), 6.75 (d, $J = 3.0$ Hz, 1H), 6.69 (dd, $J = 8.7, 3.0$ Hz, 1H), 0.98 (s, 9H), 0.82 (s, 9H), 0.18 (s, 6H), -0.09 (s, 6H).

^{13}C NMR (101 MHz, CDCl_3): $\delta = 150.01, 146.78, 138.12, 132.70, 131.53, 131.09, 121.82, 121.16, 121.02, 119.91, 25.86, 25.78, 18.32, 18.19, -4.29, -4.43$.

HRMS (NSI): m/z $[\text{M} + \text{H}]^+$ calcd for $\text{C}_{24}\text{H}_{38}\text{O}_2\text{BrSi}_2$: 493.1588; found: 493.1584.

Anal. Calcd for $\text{C}_{24}\text{H}_{37}\text{O}_2\text{BrSi}_2$: C, 58.40; H, 7.56. Found: C, 58.29; H, 7.59.

4'-bromo-1-((triisopropylsilyl)oxy)-[1,1'-biphenyl]-4(1H)-one (1d)

To a solution of **1a** (200.0 mg, 0.754 mmol, 1 equiv.) in DMF (10 mL) 2,6-lutidine (0.527 mL, 4.52 mmol, 6 equiv.) was added, followed by triisopropylsilyl trifluoromethanesulfonate (1.01 mL, 3.77 mmol, 5 equiv., CAS: 80522-42-5). The reaction mixture was stirred at 70 °C for 18 h. The reaction was quenched with saturated aqueous NaHCO_3 solution (10 mL), extracted with EtOAc (3 x 10 mL), washed with H_2O (2 x 30 mL) and concentrated in vacuo to afford an orange oil. Crude product was purified by flash chromatography (SiO_2 , *n*-pentane \rightarrow EtOAc: *n*-pentane = 3:97) to afford **4d** as a pale yellow solid (148.0 mg, 0.256 mmol, 34%), **1a** as a beige solid (72.7 mg, 0.274 mmol, 36%) and impure material which was further purified by flash chromatography (SiO_2 , *n*-pentane \rightarrow EtOAc: *n*-pentane = 1:49) to afford **1d** as a yellow oil (8.4 mg, 0.020 mmol, 3%).

Yellow oil; $R_f = 0.33$ (SiO₂, EtOAc: *n*-pentane = 1:19).

¹H NMR (400 MHz, CDCl₃): $\delta = 7.47$ (d, $J = 8.7$ Hz, 2H), 7.35 (d, $J = 8.7$ Hz, 2H), 6.82 (d, $J = 10.1$ Hz, 2H), 6.23 (d, $J = 10.1$ Hz, 2H), 1.11 – 1.05 (m, 21H).

¹³C NMR (101 MHz, CDCl₃): $\delta = 185.68, 151.53, 139.46, 131.99, 127.47, 126.88, 122.25, 73.22, 18.36, 13.43$.

HRMS (EI): m/z [M]⁺ calcd for C₂₁H₂₉O₂BrSi: 420.1115; found: 420.1123.

Anal. Calcd not performed due to an insufficient amount of the material.

((4'-bromo-[1,1'-biphenyl]-2,5-diyl)bis(oxy))bis(triisopropylsilane) (4d)

See compound **1d** for the procedure.

Pale yellow solid; $R_f = 0.57$ (SiO₂, EtOAc: *n*-pentane = 1:99); Mp 49–50 °C.

¹H NMR (400 MHz, CDCl₃): $\delta = 7.49$ (d, $J = 8.5$ Hz, 2H), 7.37 (d, $J = 8.4$ Hz, 2H), 6.79 (d, $J = 2.7$ Hz, 1H), 6.77 (d, $J = 8.5$ Hz, 1H), 6.72 (dd, $J = 8.5, 2.7$ Hz, 1H), 1.26 – 1.21 (m, 3H), 1.11 – 1.06 (m, 21H), 0.94 (d, $J = 7.2$ Hz, 18H).

¹³C NMR (101 MHz, CDCl₃): $\delta = 150.10, 147.18, 138.28, 132.24, 131.48, 131.02, 121.81, 120.92, 120.14, 119.71, 18.08, 17.96, 13.02, 12.76$.

HRMS (EI): m/z [M]⁺ calcd for C₃₀H₄₉O₂BrSi₂: 576.2449; found: 576.2467.

Anal. Calcd for C₃₀H₄₉O₂BrSi₂: C, 62.36; H, 8.55. Found: C, 62.24; H, 8.65.

4,4''-dibromo-[1,1':4',1''-terphenyl]-1',4'-diol (2a)

From *p*-benzoquinone:

We modified a literature procedure:^[61] *n*-butyllithium (2.5 M in hexanes, 14.5 mL, 36.1 mmol, 2.6 equiv., CAS: 109-72-8) was added dropwise to a solution of 1,4-dibromobenzene (9.18 g, 38.9 mmol, 2.8 equiv., CAS: 106-37-6) in THF (92 mL) at –78 °C. The reaction was stirred at this temperature for 30 min, before a solution of *p*-benzoquinone (1.50 g, 13.9 mmol, 1 equiv., CAS: 106-51-4) in THF (32 mL) was added via cannula. The resulting reaction mixture was stirred at –78 °C for 1 h and then at room temperature for 15 h. The reaction was quenched with H₂O (50 mL), diluted with Et₂O (100 mL) and extracted with Et₂O (3 x 50 mL). The organic layers were

Chapter 2

combined, washed with brine (150 mL), dried over anhydrous Na_2SO_4 , filtered and concentrated in vacuo to afford a dark oil. Crude product was purified by flash chromatography (SiO_2 , EtOAc: *n*-pentane = 1:9 \rightarrow EtOAc: *n*-pentane = 1:1) to afford **2a** as a beige solid (2.95 g, 7.0 mmol, 50%). Spectral data match the literature-reported values.^[77]

From compound **2c**:

Tetrabutylammonium fluoride (1M solution in THF, 0.161 mL, 0.161 mmol, 2.5 equiv., CAS: 429-41-4) was added to a solution of **2c** (42.0 mg, 0.065 mmol, 1 equiv.) in THF (1 mL). The reaction mixture was stirred at room temperature for 2.5 h. The reaction was quenched with H_2O (5 mL), extracted with EtOAc (3 x 5 mL) and concentrated in vacuo to afford a yellow oil. Crude product was purified by flash chromatography (SiO_2 , EtOAc: *n*-pentane = 3:7 \rightarrow EtOAc: *n*-pentane = 2:3) to afford **2a** as a white solid (19.8 mg, 0.047 mmol, 73%).

From compound **2e**:

Tetrabutylammonium fluoride (1M solution in THF, 0.384 mL, 0.384 mmol, 2.5 equiv.) was added to a solution of **2e** (100.0 mg, 0.154 mmol, 1 equiv.) in THF (2.5 mL). The reaction mixture was stirred at room temperature for 2.5 h. The reaction was quenched with H_2O (5 mL), extracted with EtOAc (3 x 5 mL) and concentrated in vacuo to afford a colorless oil. Crude product was purified by flash chromatography (SiO_2 , EtOAc: *n*-pentane = 1:9 \rightarrow EtOAc: *n*-pentane = 1:1) to afford **2a** as a white solid (53.6 mg, 0.127 mmol, 83%).

Beige solid; R_f = 0.34 (SiO_2 , EtOAc: *n*-pentane = 1:1); Mp 141–142°C.

^1H NMR (300 MHz, CD_2Cl_2): δ = 7.48 (d, J = 8.6 Hz, 4H), 7.31 (d, J = 8.6 Hz, 4H), 6.03 (s, 4H), 2.34 (s, 2H).

^{13}C NMR (101 MHz, CD_2Cl_2): δ = 143.46, 132.34, 131.97, 127.81, 121.94, 69.32.

^1H NMR (300 MHz, CDCl_3): δ = 7.48 (d, J = 8.6 Hz, 4H), 7.29 (d, J = 8.6 Hz, 4H), 6.04 (s, 4H), 2.25 (s, 2H).

HRMS (NSI): m/z [$M - \text{H}$]⁺ calcd for $\text{C}_{18}\text{H}_{13}\text{O}_2\text{Br}_2$: 418.9288; found: 418.9275.

Anal. Calcd for $\text{C}_{18}\text{H}_{14}\text{O}_2\text{Br}_2$: C, 51.22; H, 3.34. Found: C, 51.46; H, 3.36.

((4,4''-dibromo-[1,1':4',1''-terphenyl]-1',4'-diyl)bis(oxy))bis(triethylsilane) (2b)

We adapted a literature procedure:^[6] Chlorotriethylsilane (2.1 mL, 12.8 mmol, 3 equiv.) was added to a solution of **2a** (1.80 g, 4.3 mmol, 1 equiv.) and imidazole (1.16 g, 17.0 mmol, 4 equiv.) in DMF

(16 mL). The reaction mixture was stirred at 40 °C for 12 h. The reaction was quenched with saturated aqueous NaHCO₃ solution (15 mL) and extracted with EtOAc (3 x 30 mL). The organic layers were combined, washed with saturated aqueous NaHCO₃ solution (100 mL), H₂O (2 x 100 mL) and brine (100 mL), dried over anhydrous Na₂SO₄, filtered and concentrated in vacuo to afford an orange oil. Crude product was purified by flash chromatography (SiO₂, *n*-pentane → EtOAc: *n*-pentane = 1:19) to afford **2b** as a white solid (2.14 g, 3.3 mmol, 77%). Spectral data match the literature-reported values.^[61]

White solid; *R*_f = 0.35 (SiO₂, *n*-pentane); Mp 63–64 °C.

¹H NMR (400 MHz, CDCl₃): δ = 7.39 (d, *J* = 8.6 Hz, 4H), 7.18 (d, *J* = 8.7 Hz, 4H), 5.96 (s, 4H), 0.93 (t, *J* = 7.9 Hz, 18H), 0.60 (q, *J* = 7.9 Hz, 12H).

¹³C NMR (101 MHz, CDCl₃): δ = 145.11, 131.56, 131.41, 127.76, 121.46, 71.25, 7.15, 6.57.

HRMS (EI): *m/z* [M]⁺ calcd for C₃₀H₄₂O₂Br₂Si₂: 648.1085; found: 648.1103.

Anal. Calcd for C₃₀H₄₂O₂Br₂Si₂: C, 55.38; H, 6.51. Found: C, 55.35; H, 6.47.

4,4''-dibromo-4'-((triethylsilyloxy)-[1,1':4',1''-terphenyl]-1'(4'H)-ol (6b)

n-Butyllithium (2.5 M in hexanes, 0.221 mL, 0.553 mmol, 1.95 equiv.) was added dropwise to a solution of 1,4-dibromobenzene (134.0 mg, 0.567 mmol, 2 equiv.) in THF (1 mL) at –78 °C. The reaction was stirred at this temperature for 30 min, before a solution of **1b** (107.6 mg, 0.284 mmol, 1 equiv.) in THF (1 mL) was added via cannula. The resulting reaction mixture was stirred at –78 °C for 2 h. The reaction was quenched with EtOH (1 mL) and after the addition of H₂O (5 mL), the organic phases were extracted with EtOAc (3 x 10 mL). The organic layers were combined and concentrated in vacuo to afford an orange oil. Crude product was purified by flash chromatography (SiO₂, EtOAc:*n*-pentane = 1:19) to afford **6b** as a colorless oil (93.6 mg, 0.175 mmol, 62%).

Colorless oil; *R*_f = 0.16 (SiO₂, EtOAc:*n*-pentane = 1:19).

¹H NMR (400 MHz, CD₂Cl₂): δ = 7.49 (d, *J* = 8.6 Hz, 2H), 7.43 (d, *J* = 8.6 Hz, 2H), 7.32 (d, *J* = 8.6 Hz, 2H), 7.25 (d, *J* = 8.7 Hz, 2H), 6.00 (s, 4H), 0.99 (t, *J* = 7.9 Hz, 9H), 0.69 (q, *J* = 8.0 Hz, 6H).

¹³C NMR (101 MHz, CD₂Cl₂): δ = 145.29, 143.91, 133.36, 131.95, 131.66, 131.10, 127.97, 127.83, 121.95, 121.45, 71.52, 69.36, 7.20, 6.81.

Chapter 2

^1H NMR (400 MHz, CDCl_3): δ = 7.48 (d, J = 8.6 Hz, 2H), 7.42 (d, J = 8.6 Hz, 2H), 7.31 (d, J = 8.6 Hz, 2H), 7.22 (d, J = 8.6 Hz, 2H), 5.99 (d, J = 10.5 Hz, 2H), 5.97 (d, J = 10.5 Hz, 2H), 0.99 (t, J = 7.9 Hz, 9H), 0.68 (q, J = 7.9 Hz, 6H).

HRMS (EI): m/z [M] $^+$ calcd for $\text{C}_{24}\text{H}_{28}\text{O}_2\text{Br}_2\text{Si}$: 534.0220; found: 534.0232.

Anal. Calcd for $\text{C}_{24}\text{H}_{28}\text{O}_2\text{Br}_2\text{Si}$: C, 53.74; H, 5.26. Found: C, 52.2; H, 4.99.

((4,4''-dibromo-[1,1':4',1''-terphenyl]-1',4'-diyl)bis(oxy))bis(tert-butyldimethylsilane) (2c)

To a solution of **2a** (100.0 mg, 0.237 mmol, 1 equiv.) in DMF (4 mL) 2,6-lutidine (0.166 mL, 1.42 mmol, 6 equiv.) was added, followed by *tert*-butyldimethylsilyl trifluoromethanesulfonate (0.272 mL, 1.18 mmol, 5 equiv.). The reaction mixture was stirred at 50 °C for 18 h. The reaction was quenched with saturated aqueous NaHCO_3 solution (5 mL) and extracted with EtOAc (3 x 10 mL). The organic layers were combined, washed with H_2O (2 x 30 mL) and concentrated in vacuo to afford a white solid. Crude product was purified by flash chromatography (SiO_2 , *n*-pentane) to afford **2c** as a white solid (108.1 mg, 0.166 mmol, 70%).

White solid; R_f = 0.36 (SiO_2 , *n*-pentane); Mp 161–162 °C.

^1H NMR (400 MHz, CDCl_3): δ = 7.40 (d, J = 8.6 Hz, 4H), 7.20 (d, J = 8.6 Hz, 4H), 5.96 (s, 4H), 0.94 (s, 18H), 0.04 (s, 12H).

^{13}C NMR (101 MHz, CDCl_3): δ = 145.05, 131.51, 131.44, 127.75, 121.48, 71.34, 26.00, 18.50, –2.17.

HRMS (EI): m/z [M] $^+$ calcd for $\text{C}_{30}\text{H}_{42}\text{O}_2\text{Br}_2\text{Si}_2$: 648.1085; found: 648.1107.

Anal. Calcd for $\text{C}_{30}\text{H}_{42}\text{O}_2\text{Br}_2\text{Si}_2$: C, 55.38; H, 6.51. Found: C, 55.35; H, 6.47.

tert-butyl((4,4''-dibromo-[1,1':3',1''-terphenyl]-4'-yl)oxy)dimethylsilane (5c)

From compound **2a**:

To a solution of **2a** (25.0 mg, 0.059 mmol, 1 equiv.) in DMF (1 mL) 2,6-lutidine (0.083 mL, 0.710 mmol, 12 equiv.) was added, followed by *tert*-butyldimethylsilyl trifluoromethanesulfonate (0.136 mL, 0.592 mmol, 10 equiv.). The reaction mixture was stirred at 100 °C for 18 h. The reaction was quenched with saturated aqueous NaHCO_3 solution (5 mL), extracted with EtOAc (3 x 10 mL), washed with H_2O (2 x 30 mL) and concentrated in vacuo to afford a brown solid. Crude product

was purified by flash chromatography (SiO₂, *n*-pentane → EtOAc: *n*-pentane = 1:99) to afford **5c** as a white solid (23.3 mg, 0.045 mmol, 76%).

From compound **2c** with TBDMSOTf:

tert-Butyldimethylsilyl trifluoromethanesulfonate (0.177 mL, 0.768 mmol, 10 equiv.) was added to a solution of **2c** (50.0 mg, 0.077 mmol, 1 equiv.) in DMF (2 mL). The reaction mixture was stirred at 100 °C for 18 h. The reaction was quenched with saturated aqueous NaHCO₃ solution (5 mL), extracted with EtOAc (3 x 10 mL), washed with H₂O (2 x 30 mL) and concentrated in vacuo to afford a colorless waxy solid. Crude product was purified by flash chromatography (SiO₂, *n*-pentane) to afford **5c** as a white solid (32.1 mg, 0.064 mmol, 83%).

From compound **2c** with TfOH:

Triflic acid (0.08 M in DMF, 0.096 mL, 0.1 equiv., CAS: 1493-13-6) was added to a solution of **2c** (50.0 mg, 0.077 mmol, 1 equiv.) in DMF (2 mL). The reaction mixture was stirred at 100 °C for 18 h. The reaction was quenched with saturated aqueous NaHCO₃ solution (5 mL), extracted with EtOAc (3 x 10 mL), washed with H₂O (2 x 30 mL) and concentrated in vacuo to afford a white solid. Crude product was purified by flash chromatography (SiO₂, *n*-pentane → EtOAc: *n*-pentane = 1:19) to afford **5c** as a white solid (32.4 mg, 0.065 mmol, 84%).

White solid; *R*_f = 0.26 (SiO₂, *n*-pentane); Mp 101–102 °C.

¹H NMR (400 MHz, CDCl₃): δ = 7.54 (d, *J* = 8.6 Hz, 2H), 7.53 (d, *J* = 8.5 Hz, 2H), 7.46 – 7.39 (m, 6H), 6.97 (d, *J* = 8.4 Hz, 1H), 0.85 (s, 9H), 0.02 (s, 6H).

¹³C NMR (101 MHz, CDCl₃): δ = 152.59, 139.65, 137.93, 133.62, 132.74, 131.99, 131.56, 131.21, 129.30, 128.50, 127.23, 121.28, 121.20, 120.96, 25.73, 18.26, -4.29.

HRMS (EI): *m/z* [M]⁺ calcd for C₂₄H₂₆OBr₂Si: 516.0114; found: 516.0118.

Anal. Calcd for C₂₄H₂₆OBr₂Si: C, 55.61; H, 5.06. Found: C, 55.73; H, 5.26.

4,4''-dibromo-4'-((*tert*-butyldimethylsilyl)oxy)-[1,1':4',1''-terphenyl]-1'(4'*H*)-ol (6c**)**

With TBAF:

Tetrabutylammonium fluoride (1M solution in THF, 0.231 mL, 0.231 mmol, 1.5 equiv.) was added to a solution of **2e** (100.0 mg, 0.154 mmol, 1 equiv.) in THF (5 mL) at -45 °C. The reaction mixture was stirred at this temperature for 2.5 h. The reaction was quenched with H₂O (5 mL), extracted with EtOAc (3 x 5 mL) and concentrated in vacuo to afford a colorless oil. Crude product was

Chapter 2

purified by flash chromatography (SiO₂, EtOAc:*n*-pentane = 1:19 → EtOAc: *n*-pentane = 1:9) to afford **6c** as a white solid (62.9 mg, 0.117 mmol, 76%).

With K₂CO₃:

A solution of **2e** (100.0 mg, 0.154 mmol, 1 equiv.) and K₂CO₃ (212.0 mg, 1.54 mmol, 10 equiv., CAS: 584-08-7) in MeOH (3 mL) was stirred at 65 °C for 18 h. After cooling down to room temperature, the reaction mixture was diluted with H₂O (10 mL), extracted with EtOAc (3 x 10 mL) and concentrated in vacuo to afford a colorless oil. Crude product was purified by flash chromatography (SiO₂, EtOAc: *n*-pentane = 1:9) to afford **6c** as a white solid (67.7 mg, 0.126 mmol, 82%).

White solid; *R*_f = 0.15 (SiO₂, EtOAc: *n*-pentane = 1:19); Mp 63–64 °C.

¹H NMR (400 MHz, CD₂Cl₂): δ = 7.49 (d, *J* = 8.6 Hz, 2H), 7.43 (d, *J* = 8.6 Hz, 2H), 7.32 (d, *J* = 8.7 Hz, 2H), 7.25 (d, *J* = 8.6 Hz, 2H), 6.01 (d, *J* = 10.5 Hz, 2H), 5.99 (d, *J* = 10.5 Hz, 2H), 2.18 (s, 1H), 0.96 (s, 9H), 0.18 (s, 6H).

¹³C NMR (101 MHz, CD₂Cl₂): δ = 145.30, 143.96, 133.40, 131.96, 131.68, 131.08, 127.97, 127.84, 121.97, 121.46, 71.73, 69.44, 25.99, 18.68, -2.14.

¹H NMR (300 MHz, CDCl₃): δ = 7.49 (d, *J* = 8.6 Hz, 2H), 7.42 (d, *J* = 8.6 Hz, 2H), 7.31 (d, *J* = 8.6 Hz, 2H), 7.22 (d, *J* = 8.7 Hz, 2H), 6.00 (d, *J* = 10.1 Hz, 2H), 5.96 (d, *J* = 10.1 Hz, 2H), 2.06 (s, 1H), 0.96 (s, 9H), 0.17 (s, 6H).

HRMS (EI): *m/z* [M – H₂O]⁺ calcd for C₂₄H₂₆OBr₂Si: 516.0114; found: 516.0127.

Anal. Calcd for C₂₄H₂₈O₂Br₂Si: C, 53.74; H, 5.26. Found: C, 53.65; H, 5.24.

((4,4"-dibromo-[1,1':3',1''-terphenyl]-4'-yl)oxy)trisopropylsilane (5d)

See compound **6d** for the procedure. Alternatively, **5d** was obtained in a higher purity and yield according to the procedure below.

To a solution of **2a** (49.8 mg, 0.118 mmol, 1 equiv.) in DMF (2 mL) 2,6-lutidine (0.110 mL, 0.944 mmol, 8 equiv.) was added, followed by trisopropylsilyl trifluoromethanesulfonate (0.222 mL, 0.826 mmol, 7 equiv.). The reaction mixture was stirred at 100 °C for 16.5 h. The reaction was quenched with saturated aqueous NaHCO₃ solution (5 mL), extracted with EtOAc (3 x 10 mL), washed with H₂O (2 x 30 mL) and concentrated in vacuo to afford a yellow oil. Crude product was

purified by flash chromatography (SiO₂, *n*-pentane) to afford **5d** as a colorless oil (56.3 mg, 0.100 mmol, 85%).

Colorless oil; *R*_f = 0.24 (SiO₂, *n*-pentane).

¹H NMR (400 MHz, CDCl₃): δ = 7.53 (d, *J* = 8.7 Hz, 2H), 7.52 (d, *J* = 8.5 Hz, 2H), 7.46 – 7.38 (m, 6H), 6.98 (d, *J* = 8.4 Hz, 1H), 1.19 – 1.14 (m, 3H), 1.00 (d, *J* = 7.3 Hz, 18H).

¹³C NMR (101 MHz, CDCl₃): δ = 153.05, 139.62, 138.05, 133.01, 132.27, 131.96, 131.50, 131.11, 129.32, 128.41, 127.15, 121.18, 121.09, 119.88, 18.00, 13.10.

HRMS (EI): *m/z* [M]⁺ calcd for C₂₇H₃₂OBr₂Si: 558.0584; found: 558.0602.

Anal. Calcd for C₂₇H₃₂OBr₂Si: C, 57.86; H, 5.76. Found: C, 57.82; H, 5.58.

4,4''-dibromo-4'-((triisopropylsilyl)oxy)-[1,1':4',1''-terphenyl]-1'(4'H)-ol (**6d**)

To a solution of **2a** (100.0 mg, 0.237 mmol, 1 equiv.) in DMF (4 mL) 2,6-lutidine (0.166 mL, 1.43 mmol, 6 equiv.) was added, followed by triisopropylsilyl trifluoromethanesulfonate (0.318 mL, 1.18 mmol, 5 equiv.). The reaction mixture was stirred at 50 °C for 18 h. The reaction was quenched with saturated aqueous NaHCO₃ solution (5 mL), extracted with EtOAc (3 x 10 mL), washed with H₂O (2 x 30 mL) and concentrated in vacuo to afford a yellow oil. Crude product was purified by flash chromatography (SiO₂, *n*-pentane → EtOAc:*n*-pentane = 1:1) to afford **5d** as a colorless oil (8.1 mg, 0.015 mmol, 6%), **6d** as a colorless oil (53.0 mg, 0.092 mmol, 39%) and **2a** as a white solid (35.0 mg, 0.083 mmol, 35%).

Colorless oil; *R*_f = 0.53 (SiO₂, EtOAc: *n*-pentane = 1:9).

¹H NMR (300 MHz, CD₂Cl₂): δ = 7.48 (d, *J* = 8.7 Hz, 2H), 7.43 (d, *J* = 8.7 Hz, 2H), 7.30 (d, *J* = 8.7 Hz, 2H), 7.28 (d, *J* = 8.7 Hz, 2H), 6.05 (d, *J* = 10.3 Hz, 2H), 6.00 (d, *J* = 10.2 Hz, 2H), 2.14 (s, 1H), 1.19 – 1.12 (m, 3H), 1.09 (d, *J* = 5.2 Hz, 18H).

¹³C NMR (101 MHz, CD₂Cl₂): δ = 145.41, 143.73, 133.33, 131.93, 131.65, 131.07, 128.02, 127.95, 121.95, 121.49, 71.68, 69.34, 18.63, 13.78.

¹H NMR (300 MHz, CDCl₃): δ = 7.48 (d, *J* = 8.6 Hz, 2H), 7.42 (d, *J* = 8.6 Hz, 2H), 7.29 (d, *J* = 8.7 Hz, 2H), 7.26 (d, *J* = 9.4 Hz, 2H), 6.01 (d, *J* = 10.1 Hz, 2H), 5.99 (d, *J* = 10.1 Hz, 2H), 1.19 – 1.12 (m, 3H), 1.09 (d, *J* = 5.0 Hz, 18H).

HRMS (EI): *m/z* [M – H₂O]⁺ calcd for C₂₇H₃₂OBr₂Si: 558.0584; found: 558.0602.

Anal. Calcd for C₂₇H₃₄O₂Br₂Si: C, 56.06; H, 5.92. Found: C, 56.06; H, 5.86.

tert-butyl((4,4"-dibromo-4'-((triethylsilyl)oxy)-[1,1':4',1''-terphenyl]-1'(4'H)-yl)oxy)dimethylsilane (2e)

n-Butyllithium (2.5 M in hexanes, 2.62 mL, 6.55 mmol, 1.95 equiv.) was added dropwise to a solution of 1,4-dibromobenzene (1.58 g, 6.72 mmol, 2 equiv.) in THF (13 mL) at -78 °C. The reaction was stirred at this temperature for 30 min, before a solution of **1c** (1.27 g, 3.36 mmol, 1 equiv.) in THF (13 mL) was added via cannula. The resulting reaction mixture was stirred at -78 °C for 2 h. The reaction was quenched with MeOH (20 mL) and the solvents were removed in vacuo. To the residue was added H₂O (15 mL), the organic phases were extracted with CH₂Cl₂ (3 x 20 mL). The organic layers were combined and concentrated in vacuo to afford an orange oil which was used in the next step without further purification.

Chlorotriethylsilane (1.69 mL, 10.10 mmol, 3 equiv.) was added to a solution of the obtained oily crude product and imidazole (0.686 g, 10.10 mmol, 3 equiv.) in DMF (13 mL). The reaction mixture was stirred at room temperature for 17 h. The reaction was quenched with saturated aqueous NaHCO₃ solution (10 mL) and extracted with EtOAc (3 x 20 mL). The organic layers were combined, washed with H₂O (2 x 50 mL), brine (50 mL), dried over anhydrous Na₂SO₄ and concentrated in vacuo to afford a yellow oil. Crude product was purified by flash chromatography (SiO₂, *n*-pentane) to afford **2e** as a white solid (1.71 g, 3.36 mmol, 78%).

White solid; *R*_f = 0.32 (SiO₂, *n*-pentane); Mp 68–69 °C.

¹H NMR (400 MHz, CDCl₃): δ = 7.41 (d, *J* = 8.7 Hz, 2H), 7.39 (d, *J* = 8.7 Hz, 2H), 7.20 (d, *J* = 8.7 Hz, 2H), 7.17 (d, *J* = 8.7 Hz, 2H), 5.98 (d, *J* = 10.2 Hz, 2H), 5.94 (d, *J* = 10.2 Hz, 2H), 0.96 – 0.92 (m, 18H), 0.62 (q, *J* = 7.9 Hz, 6H), 0.01 (s, 6H).

¹³C NMR (101 MHz, CDCl₃): δ = 145.11, 145.06, 131.63, 131.45, 131.41, 131.41, 127.82, 127.69, 121.52, 121.41, 71.30, 71.28, 25.96, 18.50, 7.17, 6.57, -2.27.

HRMS (EI): *m/z* [M]⁺ calcd for C₃₀H₄₂O₂Br₂Si₂: 648.1085; found: 648.1105.

Anal. Calcd for C₃₀H₄₂O₂Br₂Si₂: C, 55.38; H, 6.51. Found: C, 55.57; H, 6.56.

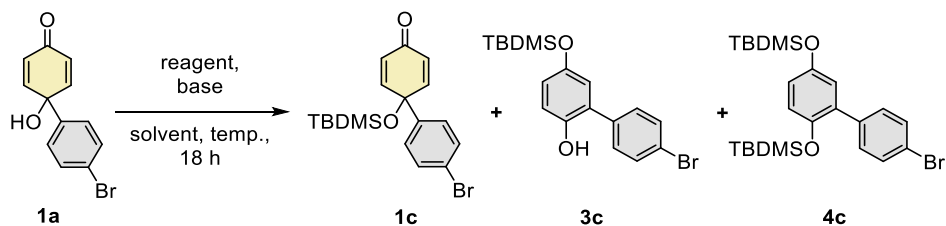
2.4.2 General procedures and optimization tables

2.4.2.1 Analysis of reaction mixtures

General procedure: After the indicated reaction time (generally 18 h), an aliquot of the reaction mixture (50–100 μL) was withdrawn with a syringe and injected to a test tube containing saturated aqueous NaHCO_3 solution and EtOAc. The organic phase was then extracted with a pipette and concentrated in vacuo. The concentrated material was analyzed by ^1H NMR in CDCl_3 and the ratios were determined through integration of selected signals.

2.4.2.2 Protection of **1a** with TBDMS group (Main text, Table 2.1, reaction A)

General procedure (as in Table S2.1, entry 6): To a solution of **1a** (25.0 mg, 0.094 mmol, 1 equiv.) in DMF (1.25 mL, $c = 0.075$ M) was added 2,6-lutidine (0.066 mL, 0.566 mmol, 6 equiv.) followed by *tert*-butyldimethylsilyl trifluoromethanesulfonate (0.108 mL, 0.472 mmol, 5 equiv.). The reaction mixture was stirred at room temperature for 18 h. The determination of the ratios was done through integration of the following peaks: 6.85 ppm (d, $J = 10.1$ Hz, 2H) for **1a**, 0.12 ppm (s, 6H) for **1c**, 7.60 ppm (d, $J = 8.4$ Hz, 2H) for **3c** and -0.09 (s, 6H) for **4c**.

Table S2.2. Optimization of protection of **1a** with TBDMS group.

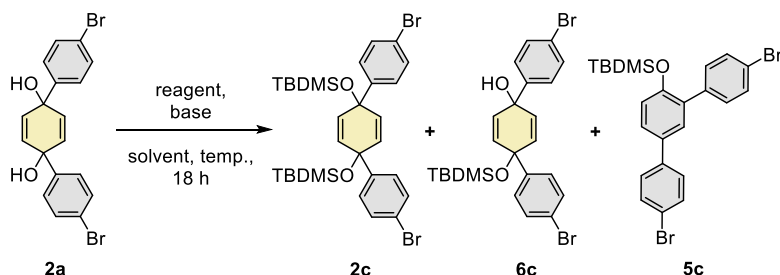
Entry	Reagent (equiv.)	Base (equiv.)	Solvent	Temp. (°C)	Ratio ^a 1a:1c:3c:4c	Yield ^b (%)		
						1c	3c	4c
1	TBDMSCl (2)	Imidazole (3)	CH ₂ Cl ₂	RT ^c	0:0:0:0 ^d	-	-	-
2	TBDMSCl (5)	Imidazole (6)	DMF	60	<100:0:0:0 ^{d,e}	-	-	-
3	TBDMSCl (5)	2,6-lutidine (6)	DMF	70	100:0:0:0	-	-	-
4 ^f	TBDMSOTf (2)	2,6-lutidine (3)	CH ₂ Cl ₂	RT	0:0:27:73	0	17	52
5 ^f	TBDMSOTf (2)	2,6-lutidine (3)	DMF	RT	80:20:0:0	-	-	-
6	TBDMSOTf (5)	2,6-lutidine (6)	DMF	RT	68:32:0:0	-	-	-
7	TBDMSOTf (5)	2,6-lutidine (6)	DMF	60	16:79:0:5	-	-	-
8	TBDMSOTf (5)	2,6-lutidine (6)	DMF	70	0:87:0:13	-	-	-
9 ^g	TBDMSOTf (5)	2,6-lutidine (6)	DMF	70	0:87:0:13	58	0	8
10	TBDMSOTf (5)	2,6-lutidine (6)	DMF	80	0:79:0:21	-	-	-
11 ^h	TBDMSOTf (2)	2,6-lutidine (6)	DMF	70	14:70:0:16	-	-	-
12 ^h	TBDMSOTf (2.5)	2,6-lutidine (6)	DMF	70	0:85:0:15	-	-	-
13 ^h	TBDMSOTf (2.5)	2,6-lutidine (3)	DMF	70	25:68:0:7	-	-	-
14 ^h	TBDMSOTf (2.5)	2,6-lutidine (4)	DMF	70	0:88:0:12	-	-	-
15 ^{g,h}	TBDMSOTf (2.5)	2,6-lutidine (4)	DMF	70	0:82:0:18	63	0	14
16 ^{f,h}	TBDMSOTf (2.5)	2,6-lutidine (4)	DMF	70	0:87:0:13	69	0	10
17 ^{h,i}	TBDMSOTf (2.5)	2,6-lutidine (4)	DMF	70	0:80:0:20	71	0	17
18	TBDMSOTf (5)	Imidazole (6)	DMF	70	29:69:0:2 ^e	-	-	-
19	TBDMSOTf (5)	NaH (6)	DMF	-50 ^o to -25 °C	<100:0:0:0 ^{d,j}	-	-	-
20	TBDMSOTf (5)	TEA (6)	DMF	70	7:79:0:14	-	-	-
21	TBDMSOTf (5)	DIPEA (6)	DMF	70	7:80:0:13	-	-	-
22	TBDMSOTf (5)	Pyridine (6)	DMF	70	0:89:0:11	-	-	-
23 ^g	TBDMSOTf (5)	DBU (6)	DMF	70	0:98:0:2	59	-	-

^a Ratio of products determined by ¹H NMR in CDCl₃ after 18 h. ^b Yield of the isolated product after 18 h. ^c RT = room temperature. ^d Formation of unidentified product(s). ^e Products ratio determined after 38 h. ^f Performed on 200 mg (0.754 mmol) scale. ^g Performed on 100 mg (0.377 mmol) scale. ^h Concentration of **1a** in DMF = 0.377 M. ⁱ Performed on 1 g (3.77 mmol) scale. ^j Products ratio determined after 4 h.

2.4.2.3 Protection of **2a** with TBDMS group (Main text, Table 2.1, reaction B)

General procedure (as in Table S2.2, entry 2): To a solution of **2a** (25.0 mg, 0.059 mmol, 1 equiv.) in DMF (1 mL, $c = 0.059$ M) was added 2,6-lutidine (0.041 mL, 0.355 mmol, 6 equiv.), followed by *tert*-butyldimethylsilyl trifluoromethanesulfonate (0.068 mL, 0.296 mmol, 5 equiv.). The reaction mixture was stirred at 70 °C for 18 h. The determination of the ratios was done through integration of the following peaks: 6.04 ppm (s, 4H) for **2a**, 0.94 ppm (s, 18H) for **2c**, 0.17 ppm (s, 6H) for **6c** and 0.85 ppm (s, 9H) for **5c**.

Table S2.2. Optimization of protection of **2a** with TBDMS group.



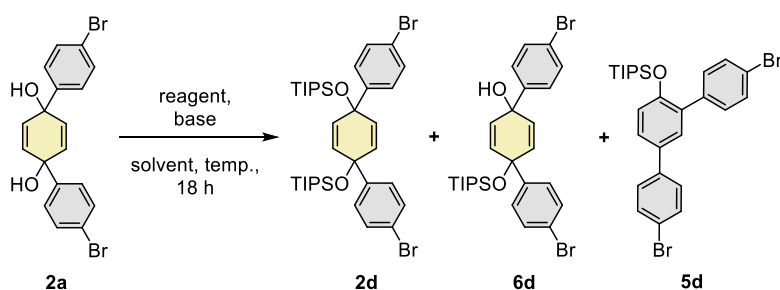
Entry	Reagent (equiv.)	Base (equiv.)	Solvent	Temp. (°C)	Ratio ^a 2a:2c:6c:5c	Yield ^b (%)		
						2c	6c	5c
1	TBDMSCl (5)	Imidazole (6)	CH ₂ Cl ₂	RT	n.c. ^c	-	-	-
	TBDMSCl (5)	Imidazole (6)	DMF	70	n.c.	-	-	-
2	TBDMSOTf (5)	2,6-lutidine (6)	DMF	70	0:52:0:48	-	-	-
3	TBDMSOTf (10)	2,6-lutidine (12)	DMF	70	0:78:0:22	-	-	-
4	TBDMSOTf (10)	2,6-lutidine (12)	DMF	100	0:4:0:96	-	-	76
5	TBDMSOTf (10)	2,6-lutidine (12)	DMF	40	0:96:0:4	-	-	-
6	TBDMSOTf (10)	2,6-lutidine (12)	DMF	RT ^d	0:90:4:6	-	-	-
7	TBDMSOTf (5)	2,6-lutidine (6)	DMF	40	0:91:4:5	-	-	-
8	TBDMSOTf (5)	2,6-lutidine (6)	DMF	50	0:93:0:7	-	-	-
9 ^e	TBDMSOTf (5)	2,6-lutidine (6)	DMF	50	0:98:0:2	70	0	<5 ^f
10 ^g	TBDMSOTf (5)	2,6-lutidine (6)	DMF	50	0:98:0:2	69	-	-
11	TBDMSOTf (5)	Imidazole (6)	DMF	50	0:41:54:5	-	-	-
12	TBDMSOTf (5)	Pyridine (6)	DMF	50	0:59:0:41	-	-	-
13	TBDMSOTf (5)	TEA (6)	DMF	50	0:93:0:7	-	-	-
14	TBDMSOTf (5)	DIPEA (6)	DMF	50	0:80:16:4	-	-	-
15	TBDMSOTf (5)	DBU (6)	DMF	50	0:0:0:0	-	-	-

^a Ratio of products determined by ¹H NMR in CDCl₃ after 18 h. ^b Yield of the isolated product after 18 h. ^c n.c. = no conversion. ^d RT = room temperature. ^e Performed on 100 mg (0.237 mmol) scale. ^f Compound **5c** was isolated along with unknown product(s). ^g Performed on 200 mg (0.474 mmol) scale.

2.4.2.4 Protection of **2a** with TIPS group (Main text, Table 2.1, reaction B)

General procedure (as in Table S2.3, entry 2): To a solution of **2a** (25.0 mg, 0.059 mmol) in DMF (1 mL, $c = 0.059$ M) was added 2,6-lutidine (0.055 mL, 0.474 mmol, 8 equiv.), followed by triisopropylsilyl trifluoromethanesulfonate (0.111 mL, 0.414 mmol, 7 equiv.). The reaction mixture was stirred at 50 °C for 18 h. The determination of the ratios was done through integration of the following peaks: 6.04 ppm (s, 4H) for **2a**, 6.05 (d, $J = 10.3$ Hz, 2H) and 6.00 (d, $J = 10.2$ Hz, 2H) for **6d** and 6.98 (d, $J = 8.4$ Hz, 1H) for **5d**.

Table S2.3. Optimization of protection of **2a** with TIPS group.



Entry	Reagent (equiv.)	Base (equiv.)	Solvent	Temp. (°C)	Ratio ^a 2a:2d:6d:5d	Yield ^b (%)		
						2d	6d	5d
1 ^c	TIPSOTf (5)	2,6-lutidine (6)	DMF	50	46:0:49:5	0	39	6 ^d
2	TIPSOTf (7)	2,6-lutidine (8)	DMF	50	29:0:63:8	-	-	-
3	TIPSOTf (10)	2,6-lutidine (12)	DMF	40/70 ^e	6:0:22:72 ^{f,g}	-	-	-
4 ^h	TIPSOTf (10)	2,6-lutidine (12)	DMF	100	0:0:0:100	0	0	85

^a Ratio of products determined by ¹H NMR in CDCl₃ after 18 h. ^b Yield of the isolated product after 18 h. ^c Performed on 100 mg (0.237 mmol) scale. ^d Additionally, **2a** was recovered in 35% yield. ^e Reaction was stirred at 40 °C for 18 h and then at 70 °C for 22 h. ^f Products ratio determined after 40 h. ^g Formation of unidentified product(s). ^h Performed on 50 mg (0.118 mmol) scale.

2.4.2.5 Stability of **2b** and **2c** (Main text, Table 2.2)

- Entries 1 and 2:

The solution of **2c** (50.0 mg, 0.077 mmol, 1 equiv.) in DMF (2 mL) was stirred at 100 °C for 18 h. After this time, the reaction mixture was analyzed by ¹H NMR according to the general procedure. Then, 2,6-lutidine (0.107 ml, 0.922 mmol, 12 equiv.) was added and the reaction mixture was stirred again at 100 °C for 18 h.

- *Entry 4:*

The solution of **2c** (25.0 mg, 0.038 mmol, 1 equiv.) and *tert*-butyldimethylsilyl chloride (57.9 mg, 0.384 mmol, 10 equiv.) in DMF (1 mL) was stirred at 100 °C for 18 h.

- For *entries* 3 and 5, see the synthesis of compound **5c**.

- *Entries* 6 and 7

To a solution of **2b** (25.0 mg, 0.038 mmol, 1 equiv.) or **2c** (25 mg, 0.038 mmol, 1 equiv.) in DMF (1 mL) was added the HCl solution. The resulting reaction mixture was stirred at 35 °C for 18 h.

Entry 6: HCl (1 mol%): 96 µL of a HCl solution (0.004 M in H₂O, 0.38 µmol, 0.01 equiv.)

Entry 7: HCl (10 mol%): 96 µL of a HCl solution (0.04 M in DMF, 0.0038 mmol, 0.1 equiv.)

- *Entries* 8 and 9

To a solution of **2b** (50.0 mg, 0.077 mmol, 1 equiv.) or **2c** (50 mg, 0.077 mmol, 1 equiv.) in DMF (2 mL) was added one of the acids listed below. The resulting reaction mixture was stirred at 35 °C for 18 h.

Entry 8: TFA (10 mol%): 96 µL of a TFA solution (0.08 M in DMF, 0.0077 mmol, 0.1 equiv.)

Entry 9: TfOH (10 mol%): 96 µL of a TfOH solution (0.08 M in DMF, 0.0077 mmol, 0.1 equiv.)

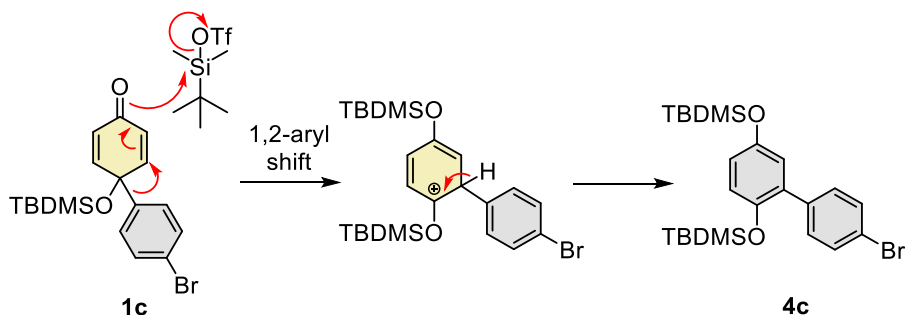
Stability of **2b**: the determination of the ratios was done by ¹H NMR through integration of the following peaks: 5.95 ppm (s, 4H) for **2b**, 5.98 ppm (s, 4H) for **6b** and 6.04 ppm (s, 4H) for **2a**.

Stability of **2c**: the determination of the ratios was done by ¹H NMR through integration of the following peaks: 0.94 ppm (s, 18H) for **2c** and 0.85 ppm (s, 9H) for **5c**.

2.4.3 Additional studies of rearrangement to **4c**

Alternatively, to the mechanism proposed for rearranged of **1a** to **3c/4c** (Main text, Scheme 2.1), an additional experiment suggests that **1c** may directly rearrange to **4c**. In fact, when **1c** was stirred with TBDMSOTf (10 equiv.) in DMF at 70 °C for 18 h, a ratio of **1c**:**4c** = 83:17 was observed. Based on this result, a new mechanism depicted on Scheme S2.1 was proposed.

Procedure: To a solution of **1c** (25.0 mg, 0.066 mmol, 1 equiv.) in DMF (1.25 mL) was added TBDMSOTf (0.151 mL, 0.659 mmol, 10 equiv.). The resulting reaction mixture was stirred at 70 °C for 18 h.



Scheme S2.1. Alternative mechanism proposed for the formation of **4c**.

2.4.4 Calculations of the bite angles

All calculations were performed with Gaussian 16 (version c.01) suite of electronic structure programs. The geometries were optimized with the respective DFT method and 6-31G(d) basis set in gas phase using default value of the density integration grid. Frequency analysis of the optimized structures was performed to confirm that the optimized geometries correspond to the local minima. For compounds **2** (Figure S2.1) with different protecting groups, a few conformations were explored to locate the lowest-energy conformation, for which the values of “bite” angles (see Figure S2.2 for definition) are reported. For structures taken from the crystals structures deposited in the Cambridge Crystal Structure Database, no conformational search was conducted because these calculations served primarily to validate the performance of the selected density functionals.

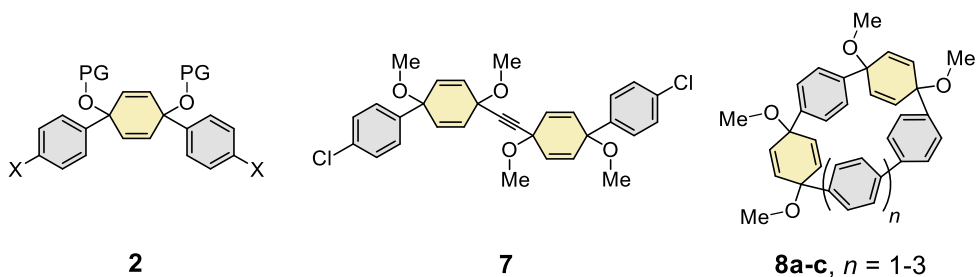


Figure S2.1. Structures of the compounds studied by DFT calculations (see Table 2.4). Compounds **2** were simplified by replacing the bromine atoms for hydrogens in position X.

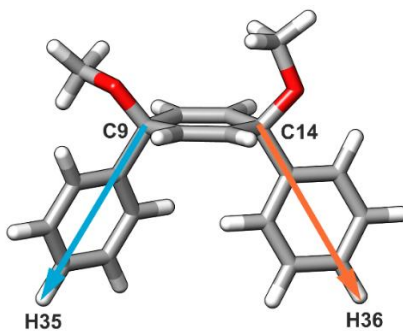


Figure S2.2. Bonding vectors in **2** are defined by atoms: C9, H35 (blue vector) and C14, H36 (orange vector). Methyl groups are shown as an example of the protecting group (see Table S2.4 for others) and the bromine atoms were replaced by hydrogens to simplify the calculations in all compounds.

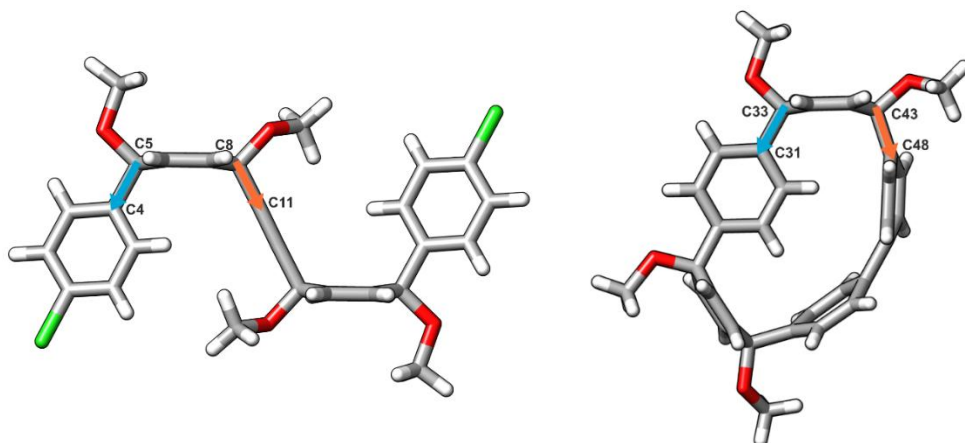
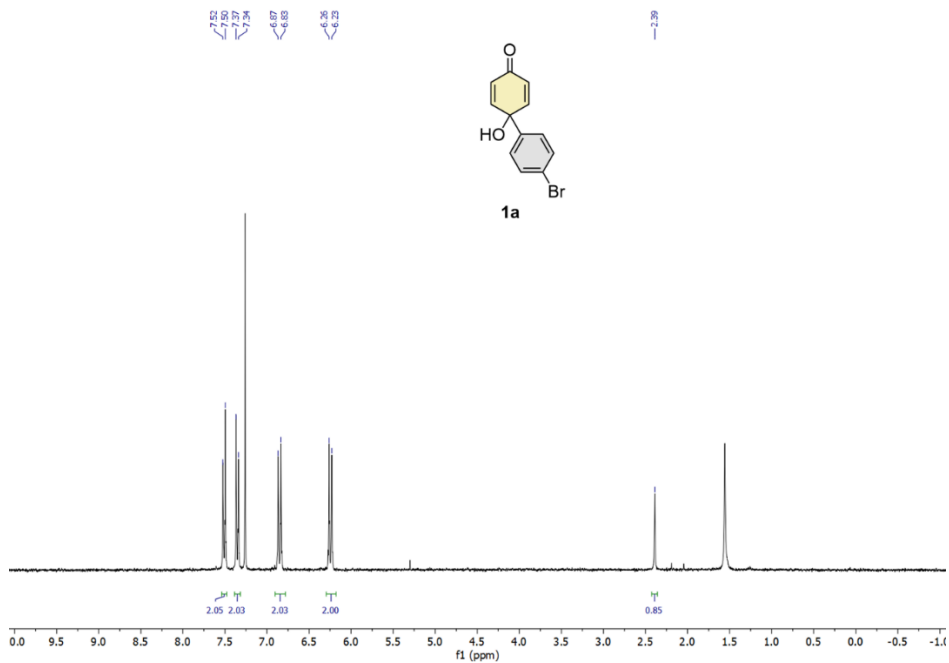


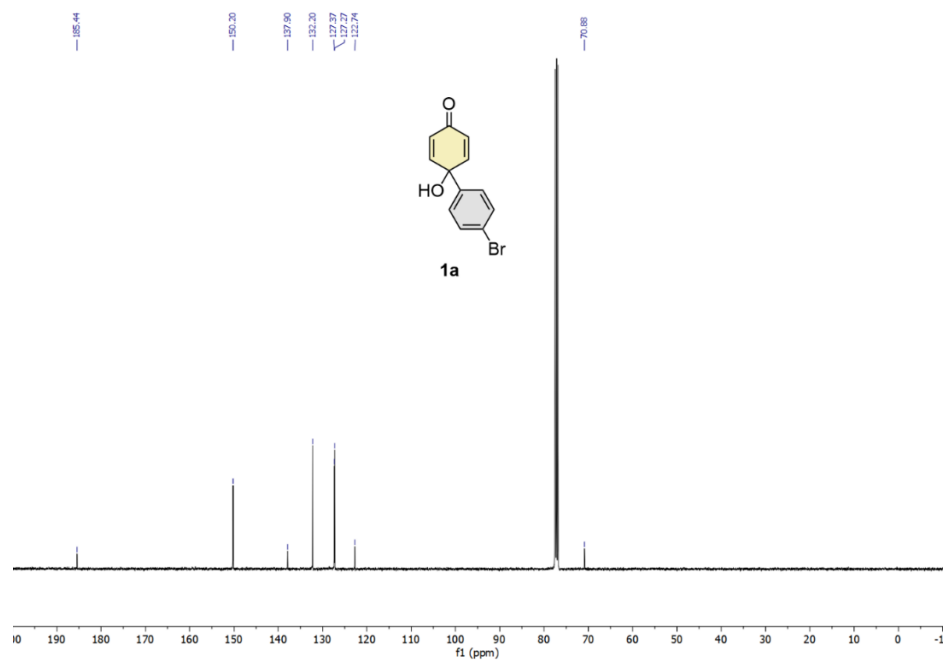
Figure S2.3. Definition of bonding vectors in **7** and **8** (Figure S2.1) to calculate the bite angle from their crystal structures and by DFT calculations.

Table S2.4. The bite angles in **2**, **7**, and **8** defined by the bonding vectors (Figure S2.2 and Figure S2.3) on the lowest-energy conformers or optimized crystal structure geometries calculated with different DFT methods using 6-31G(d) basis set. The bite angles in the parentheses are from the corresponding crystal structure geometries.

Compd.	Protecting group	Method	Bite angle (°)
2	Me	B3LYP	70.65
		MN15	65.04
		ω B97XD	61.33
	TES	B3LYP	63.57
		MN15	65.07
		ω B97XD	64.41
	TBS	B3LYP	59.58
		MN15	64.30
		ω B97XD	62.95
7	Me	B3LYP	62.32 (55.72 ^[76])
		MN15	50.90
		ω B97XD	46.10
8a (<i>n</i> = 1)	Me	B3LYP	45.22 (46.99 ^[76])
		MN15	46.22
		ω B97XD	46.33
8b (<i>n</i> = 2)	Me	B3LYP	66.29 (66.14 ^[54])
		MN15	66.53
		ω B97XD	65.70
8c (<i>n</i> = 3)	Me	B3LYP	73.72 (70.72 ^[76])
		MN15	72.20
		ω B97XD	72.31

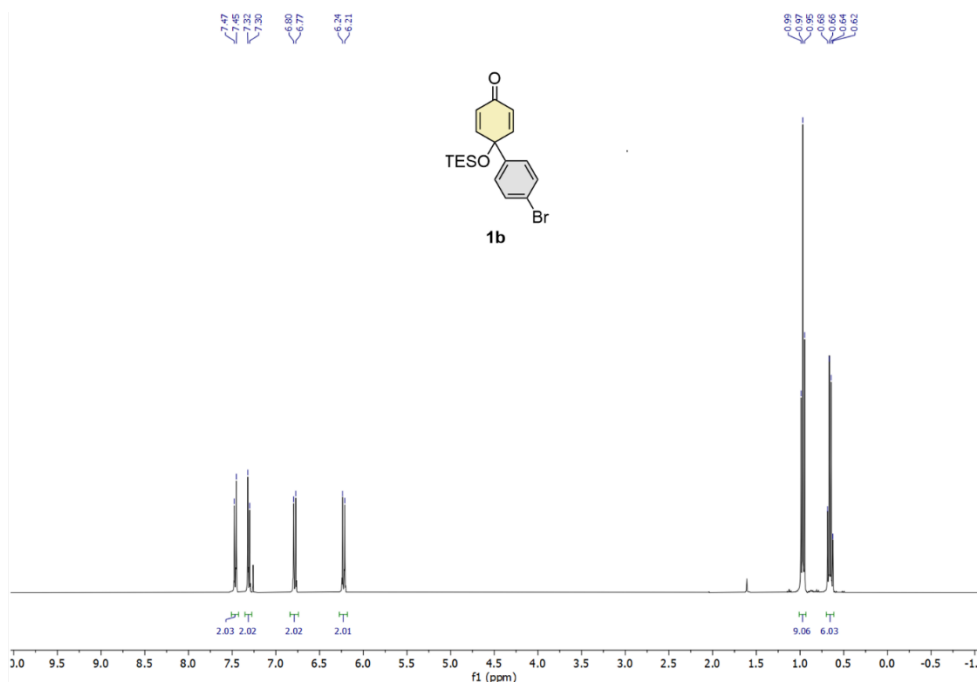
2.4.5 ^1H and ^{13}C NMR spectra

^1H NMR spectrum of compound **1a** in CDCl_3 (300 MHz).

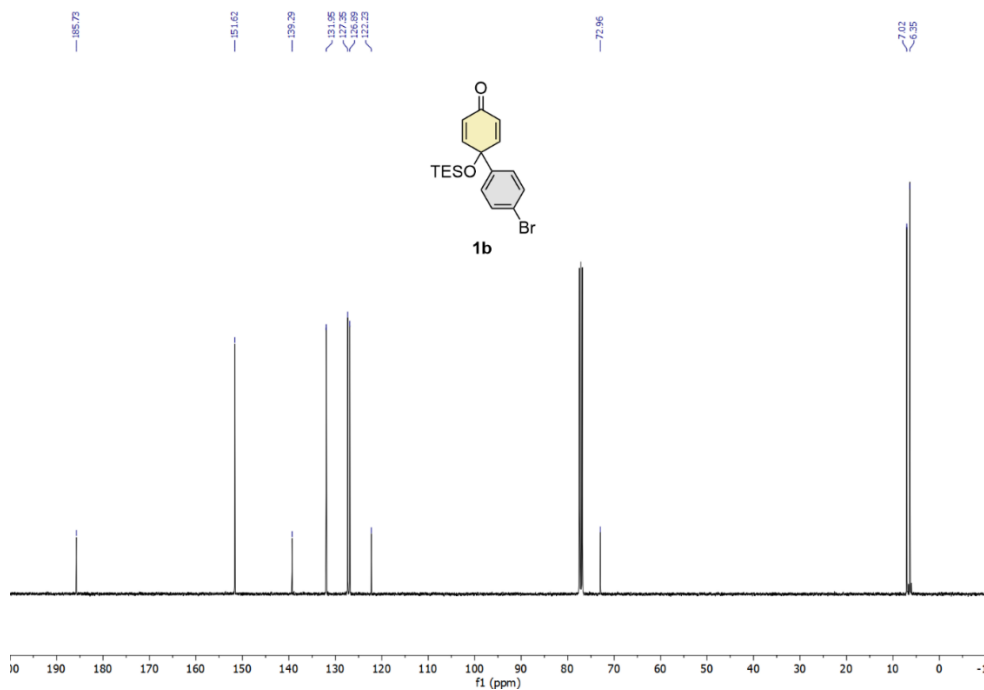


^{13}C NMR spectrum of compound **1a** in CDCl_3 (101 MHz).

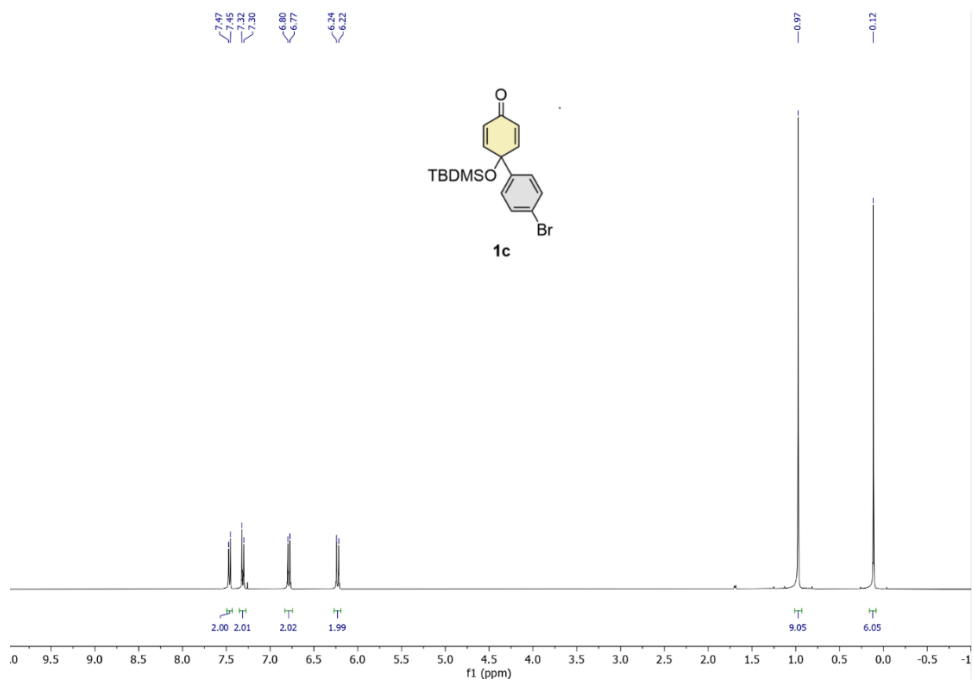
Chapter 2



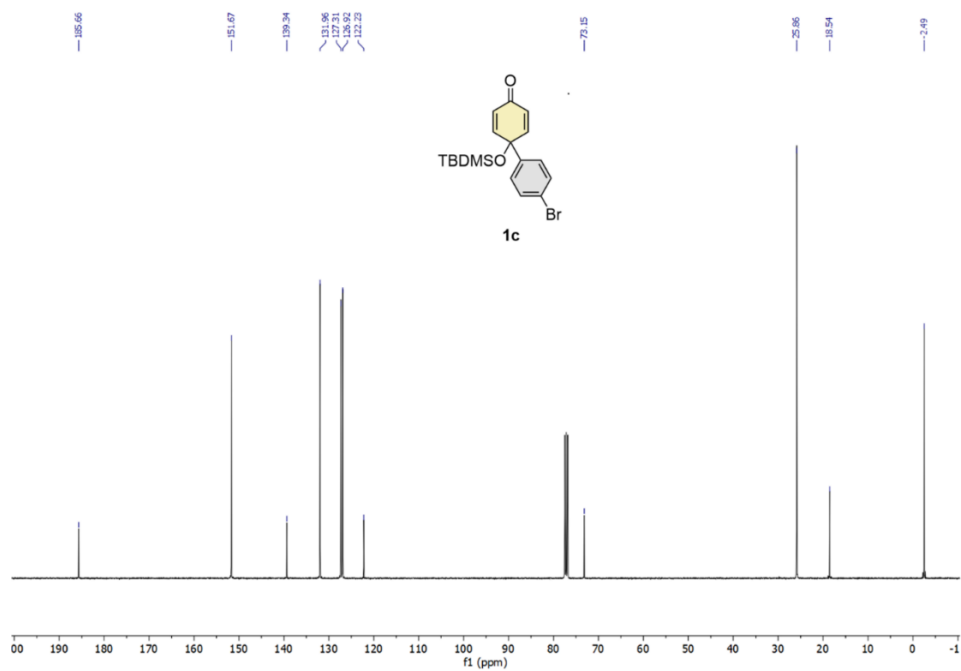
^1H NMR spectrum of compound **1b** in CDCl_3 (400 MHz).



^{13}C NMR spectrum of compound **1b** in CDCl_3 (101 MHz).

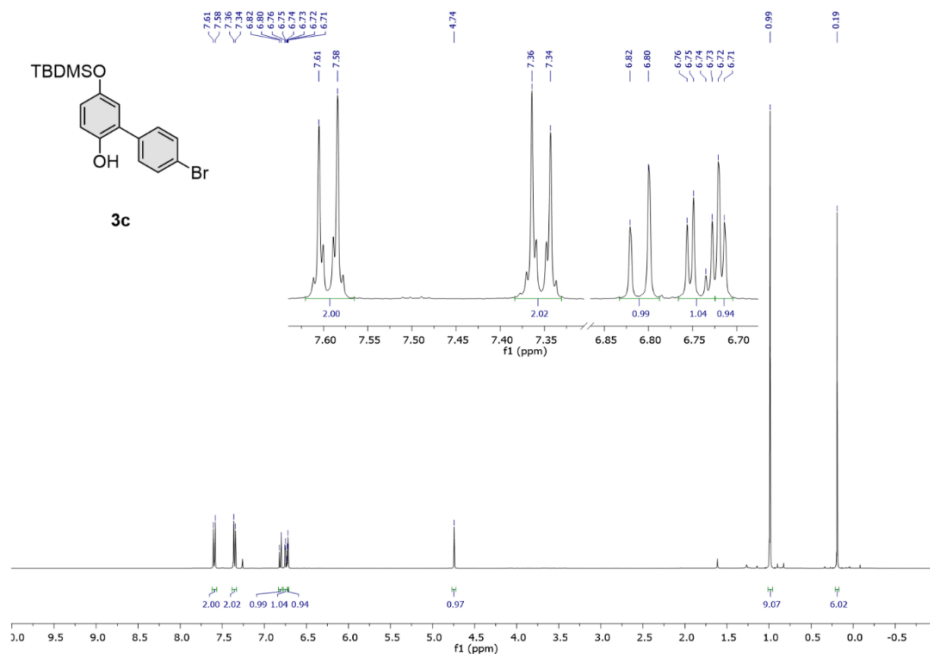


^1H NMR spectrum of compound **1c** in CDCl_3 (400 MHz).

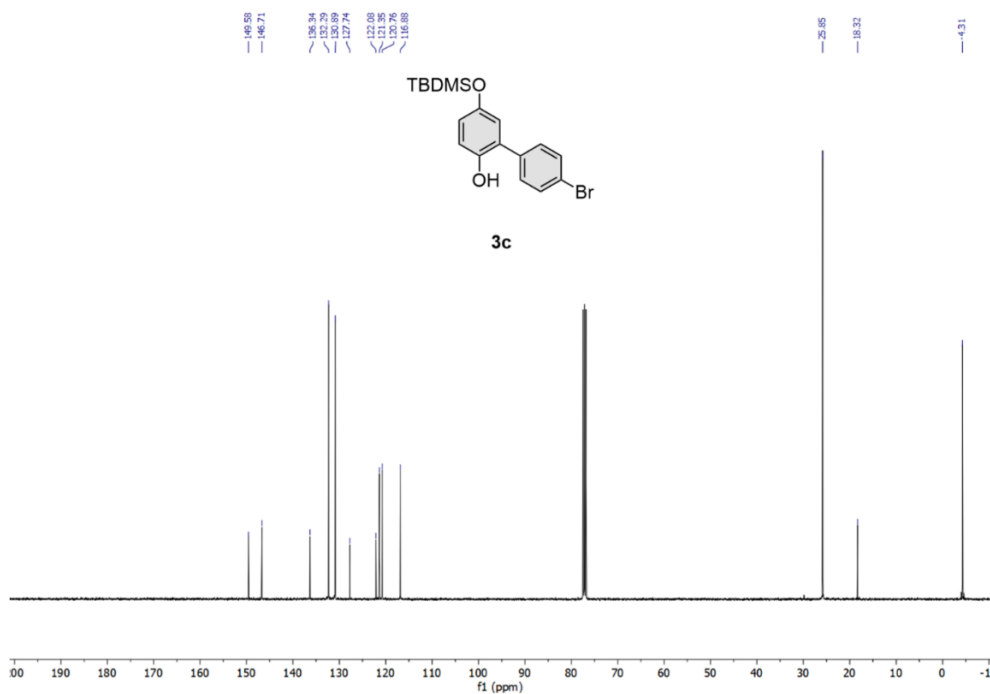


^{13}C NMR spectrum of compound **1c** in CDCl_3 (101 MHz).

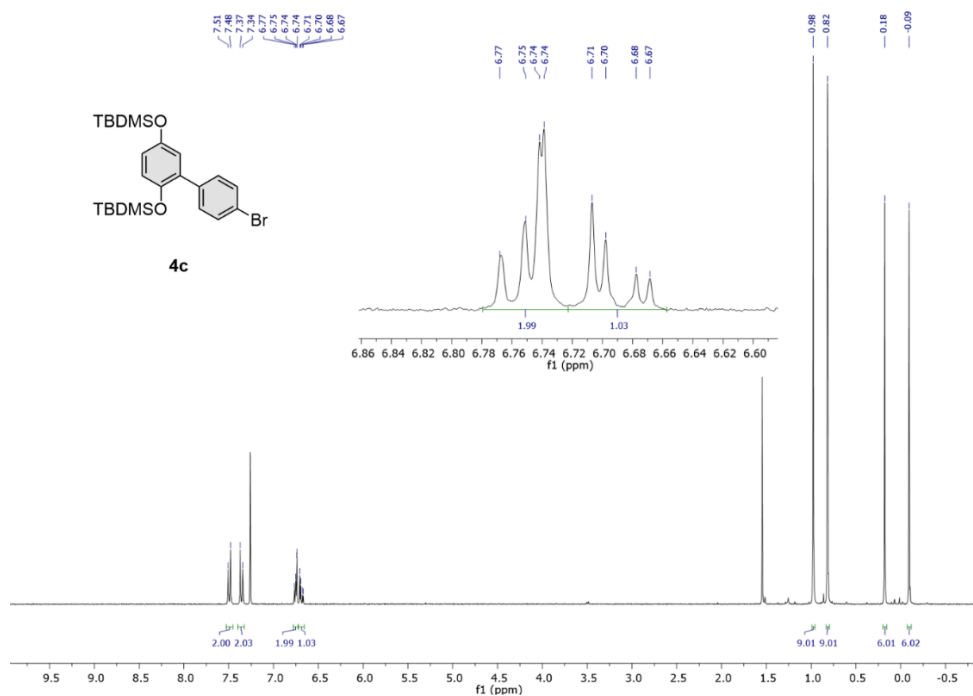
Chapter 2



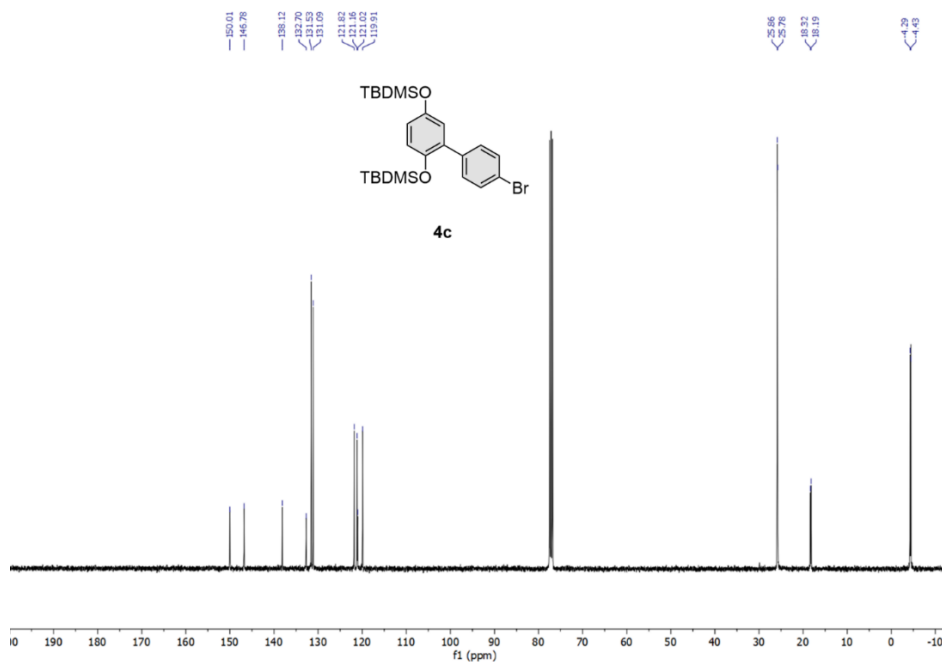
¹H NMR spectrum of compound **3c** in CDCl₃ (400 MHz).



¹³C NMR spectrum of compound **3c** in CDCl₃ (101 MHz).

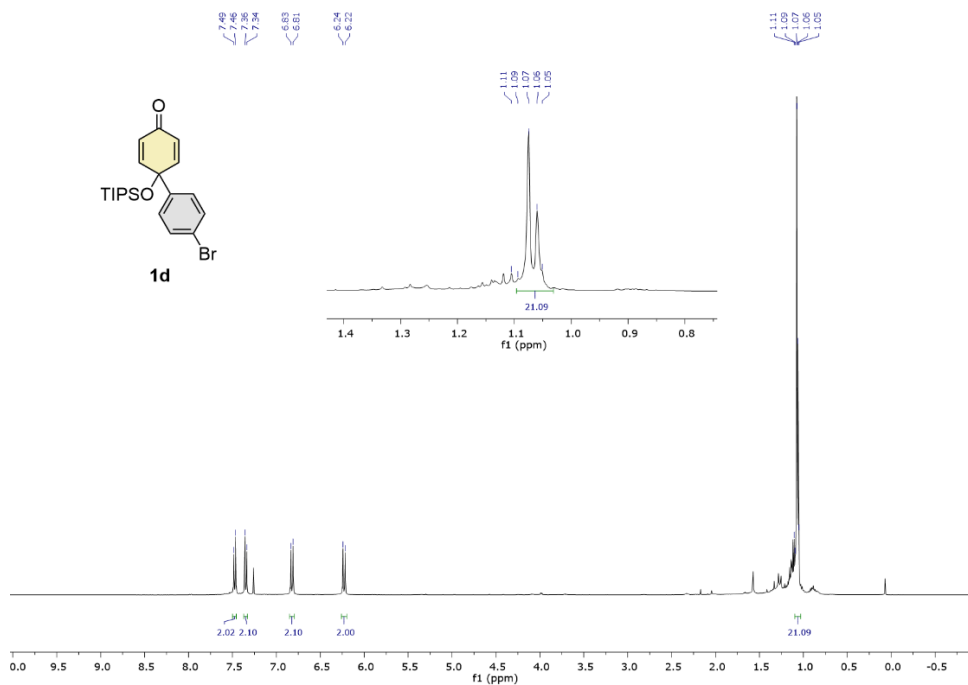


¹H NMR spectrum of compound **4c** in CDCl₃ (300 MHz).

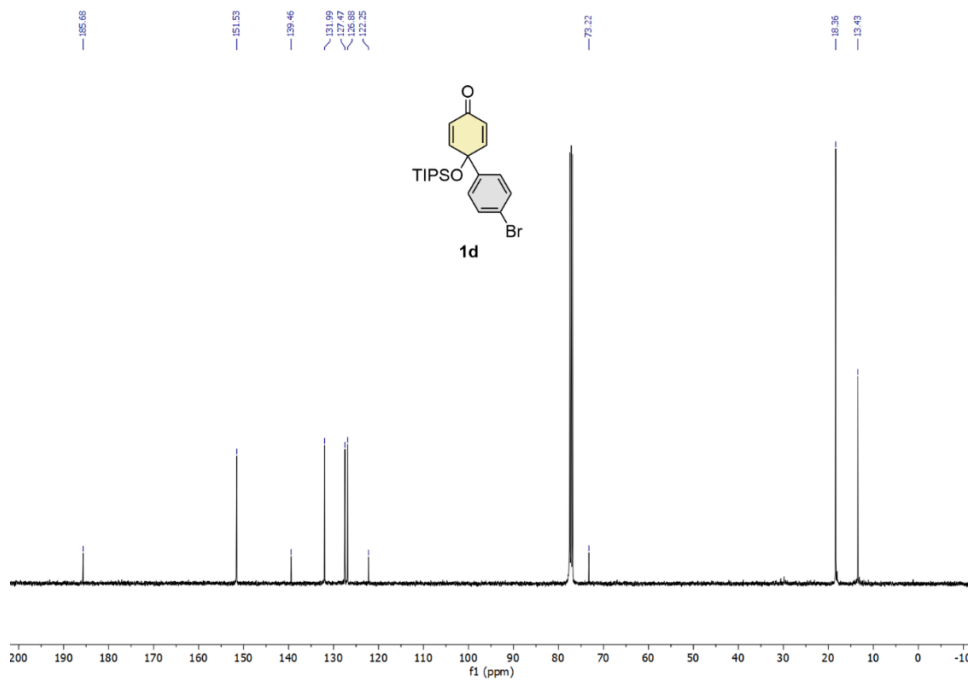


¹³C NMR spectrum of compound **4c** in CDCl₃ (101 MHz).

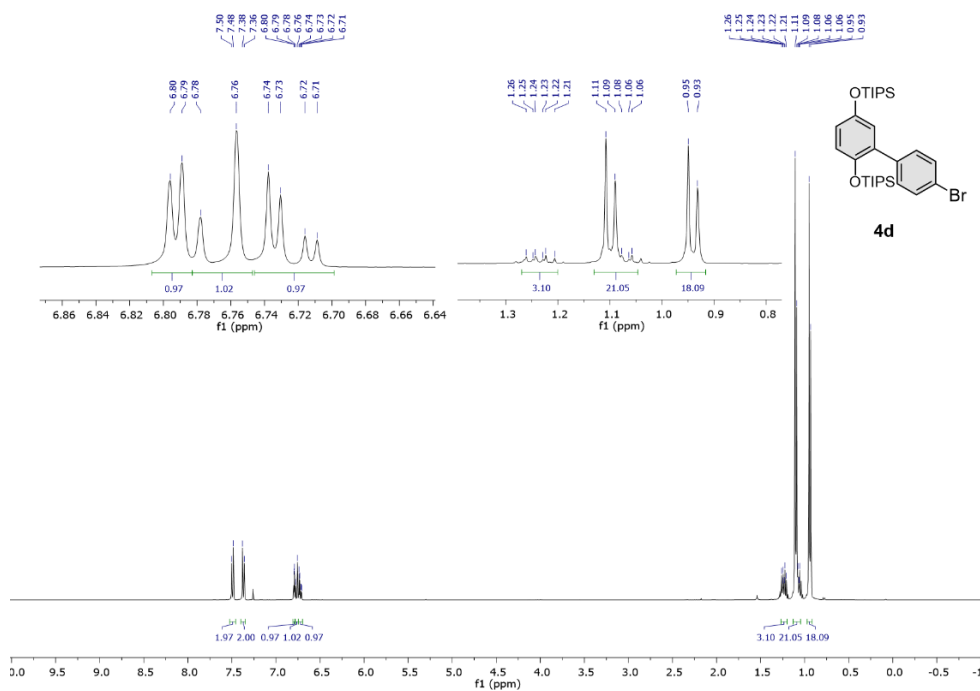
Chapter 2



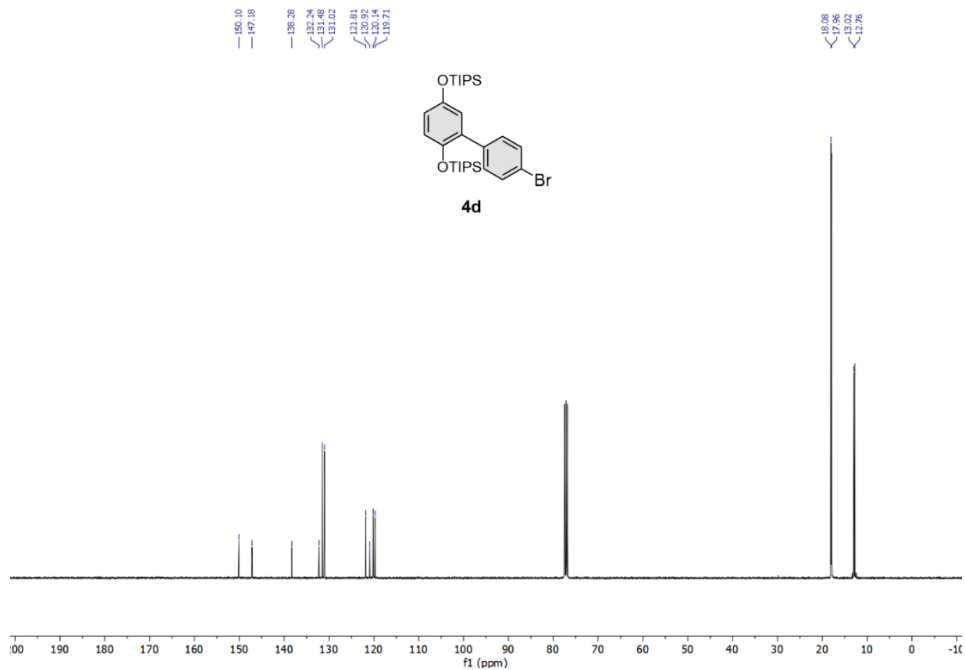
^1H NMR spectrum of compound **1d** in CDCl_3 (400 MHz).



^{13}C NMR spectrum of compound **1d** in CDCl_3 (101 MHz).

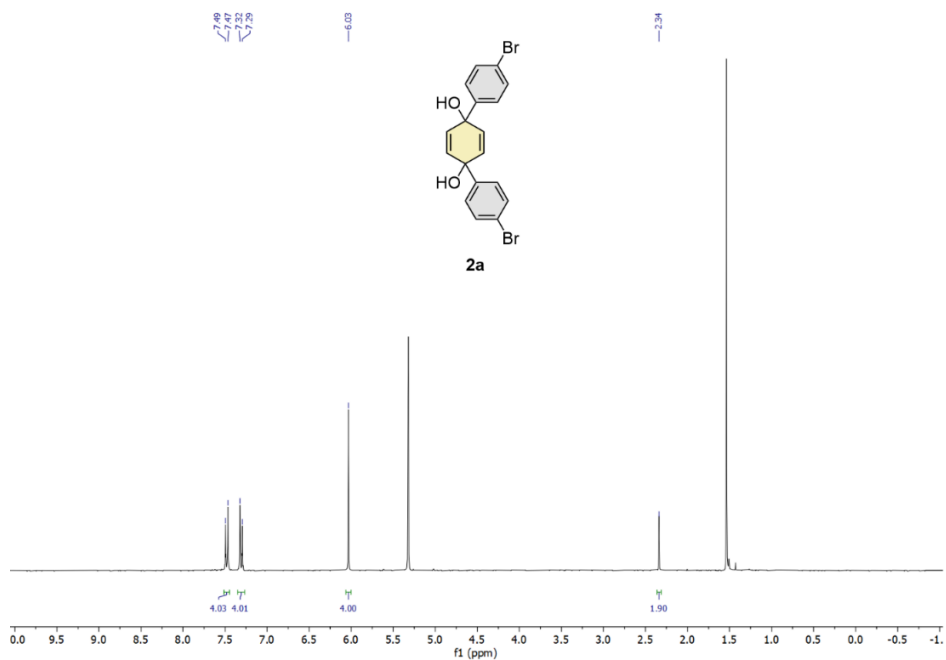


¹H NMR spectrum of compound **4d in CDCl₃ (400 MHz).**

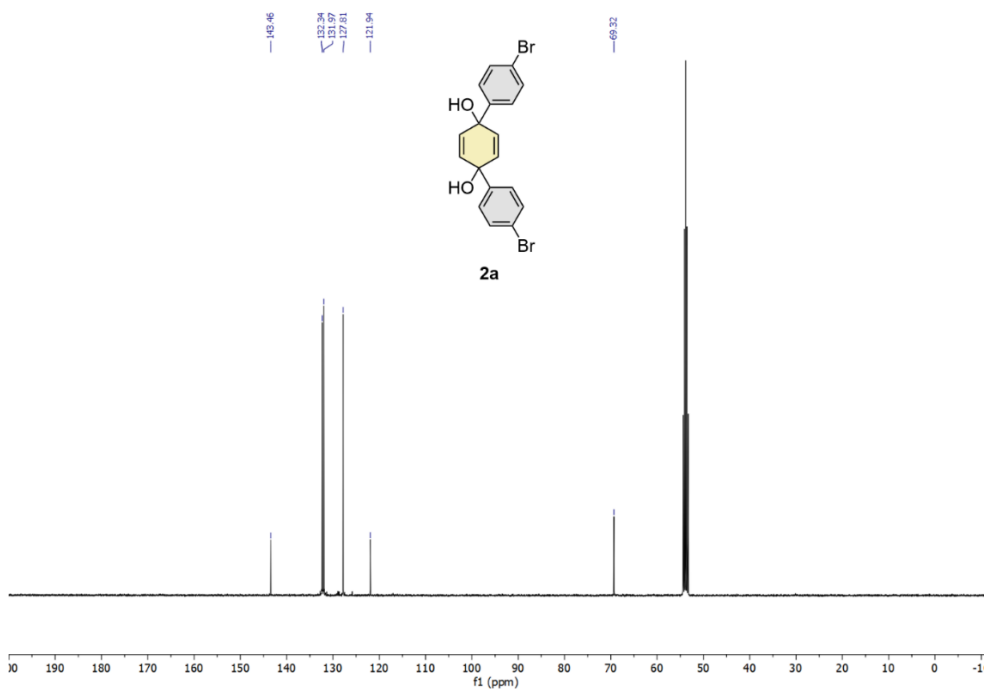


¹³C NMR spectrum of compound **4d in CDCl₃ (101 MHz).**

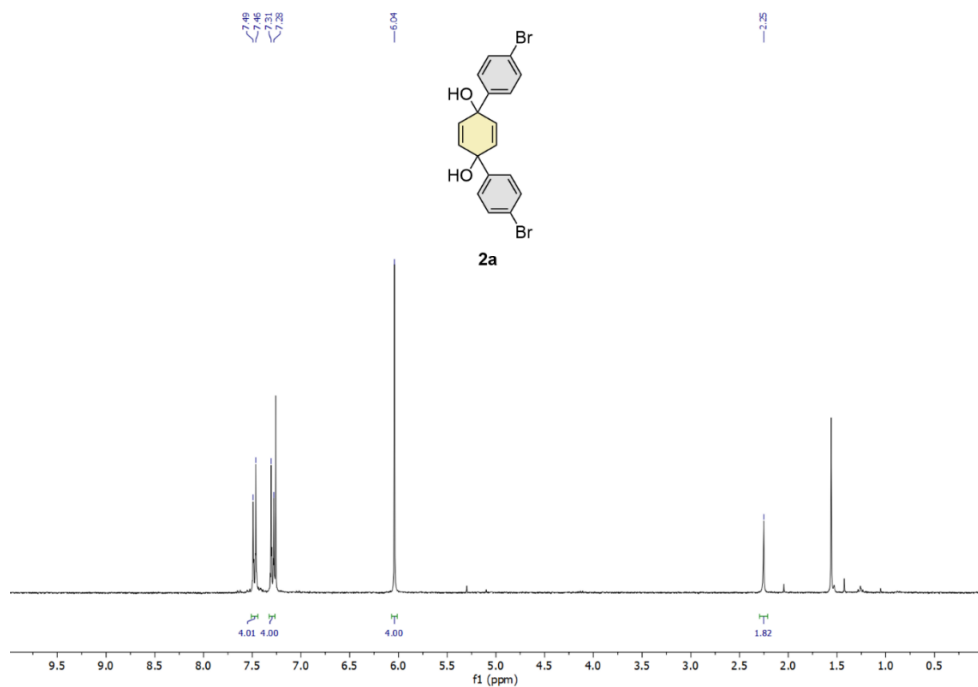
Chapter 2



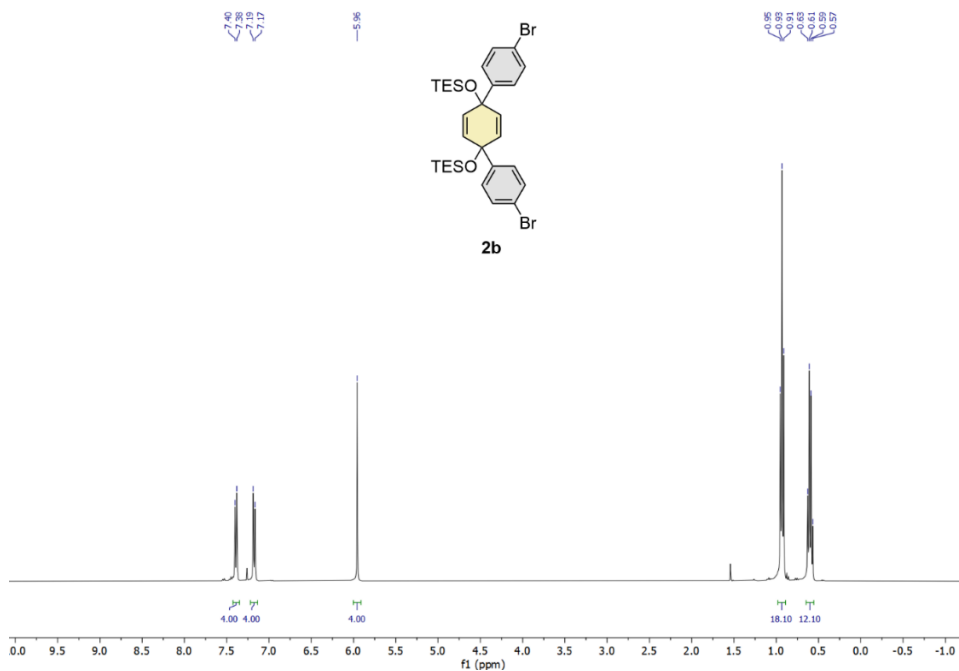
¹H NMR spectrum of compound **2a** in CD₂Cl₂ (300 MHz).



¹³C NMR spectrum of compound **2a** in CD₂Cl₂ (101 MHz).

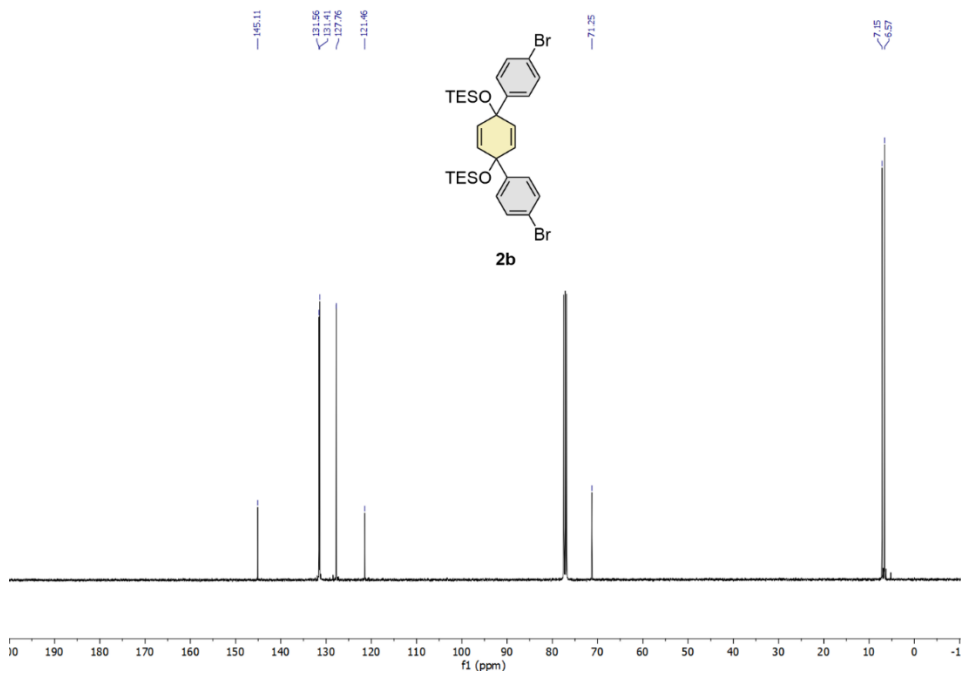


¹H NMR spectrum of compound **2a** in CDCl₃ (300 MHz).

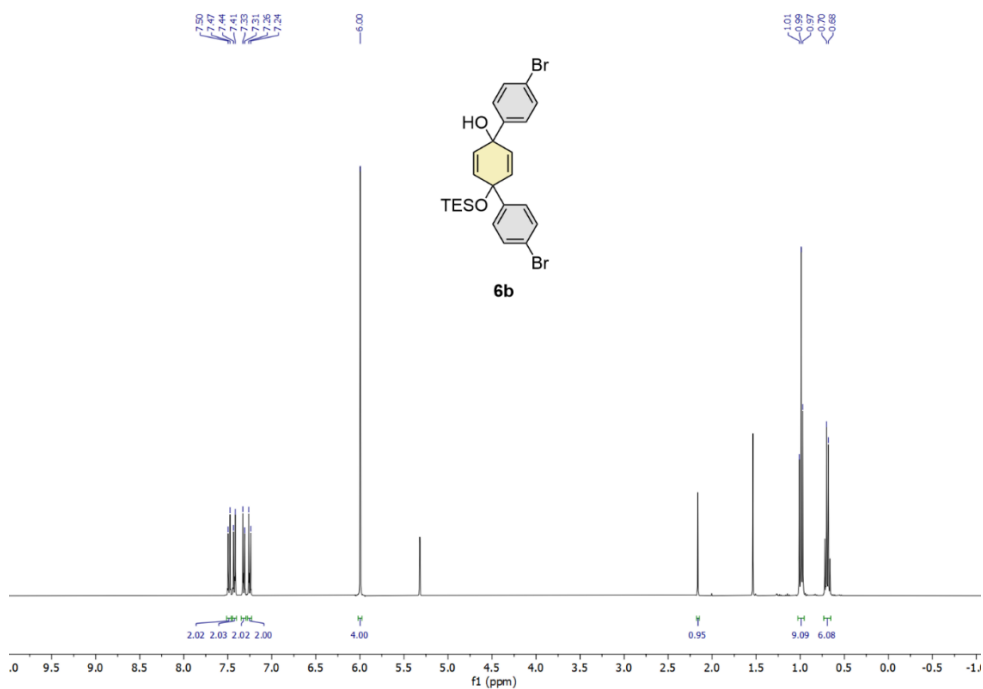


¹H NMR spectrum of compound **2b** in CDCl₃ (400 MHz).

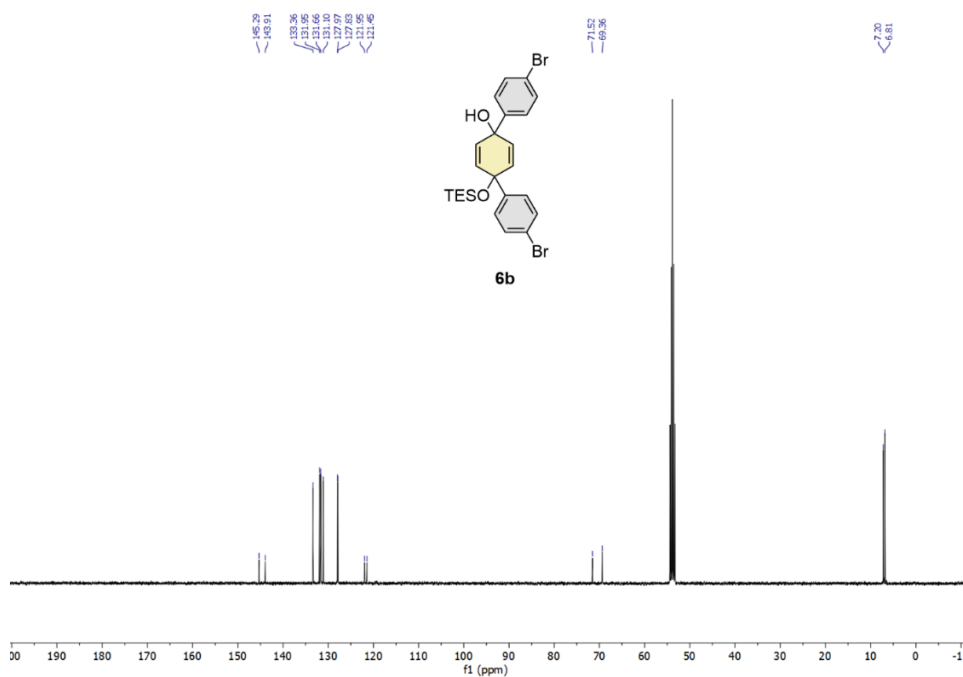
Chapter 2



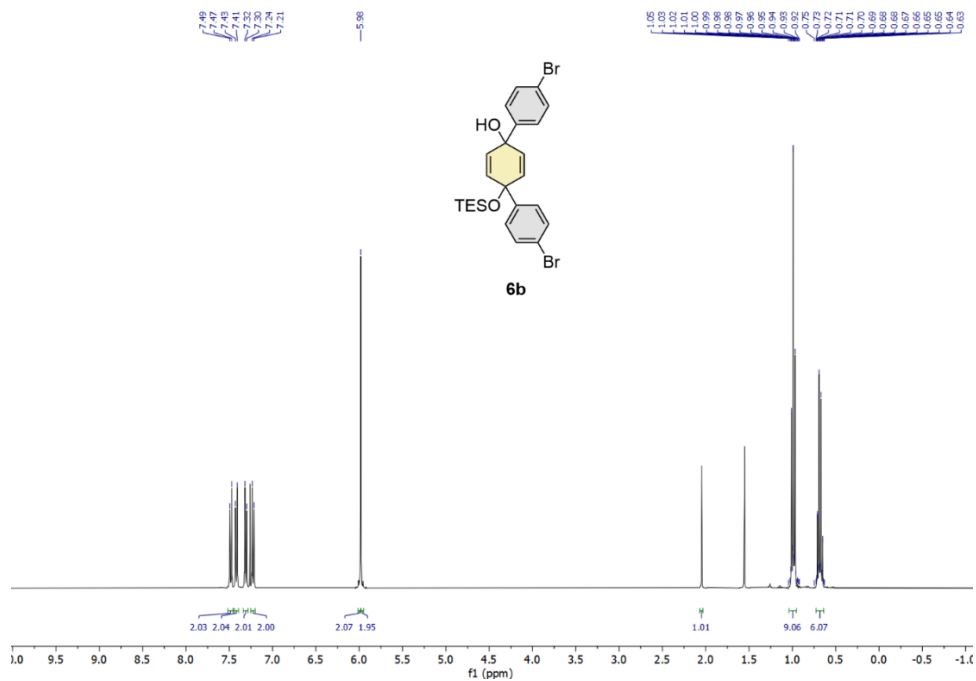
^{13}C NMR spectrum of compound **2b** in CDCl_3 (101 MHz).



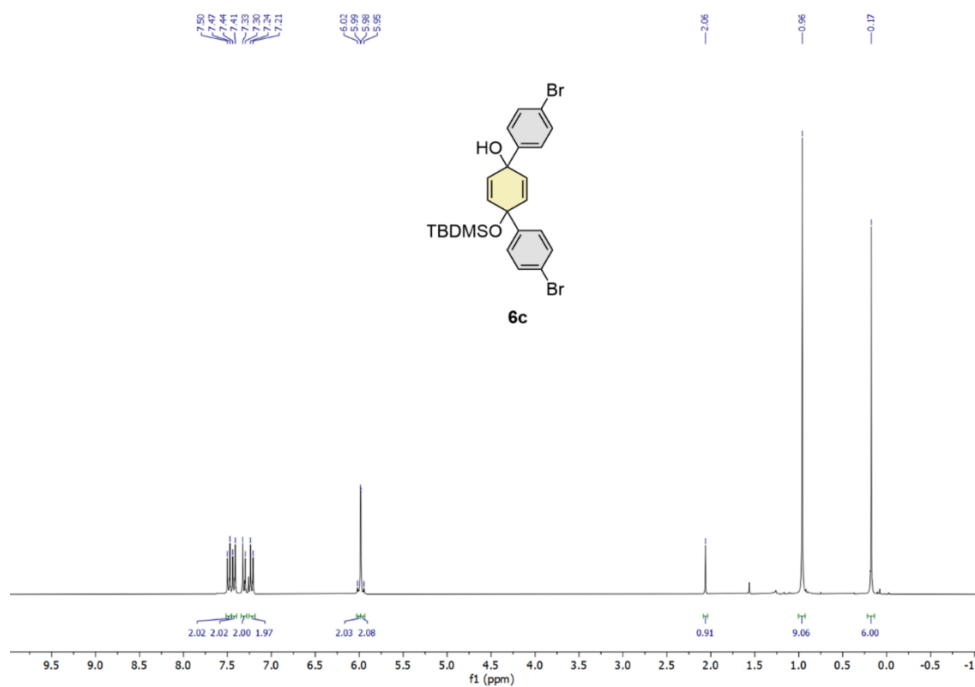
^1H NMR spectrum of compound **6b** in CD_2Cl_2 (400 MHz).



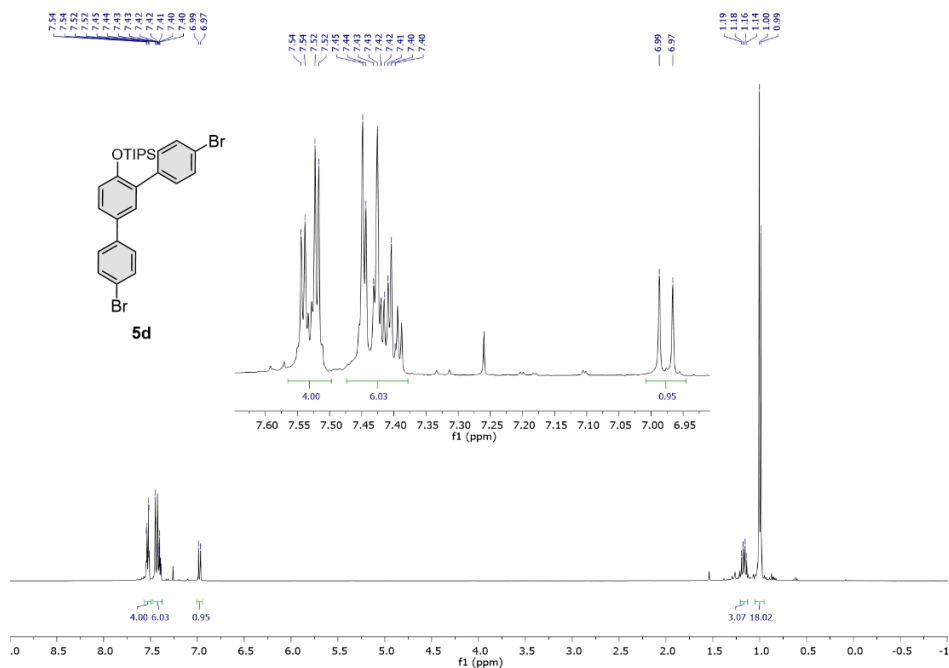
^{13}C NMR spectrum of compound **6b** in CD_2Cl_2 (101 MHz).



^1H NMR spectrum of compound **6b** in CDCl_3 (400 MHz).

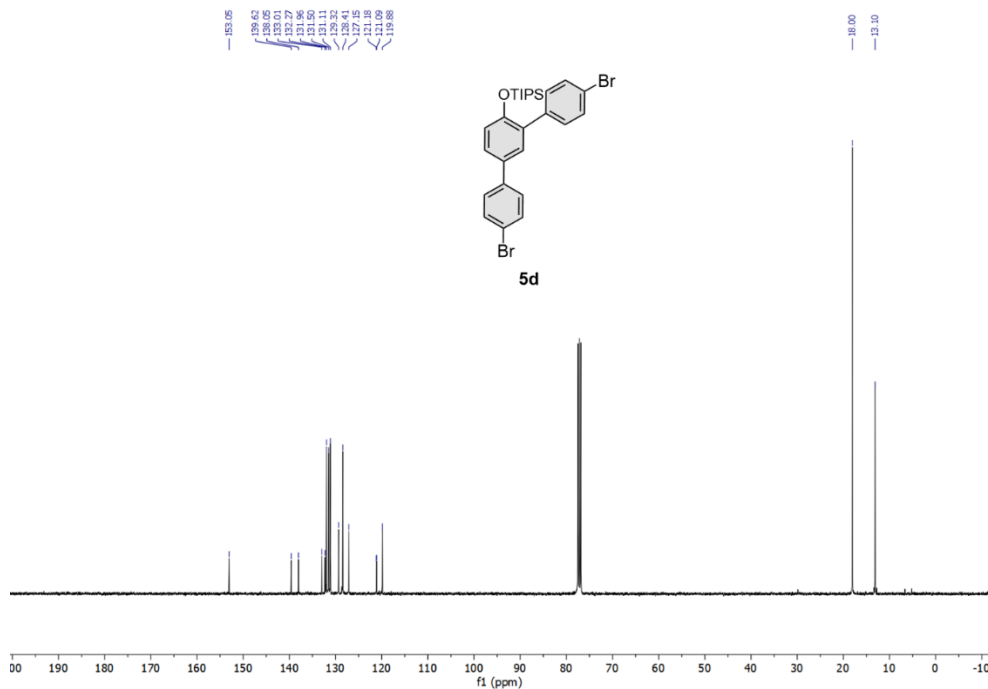


^1H NMR spectrum of compound **6c** in CDCl_3 (300 MHz).

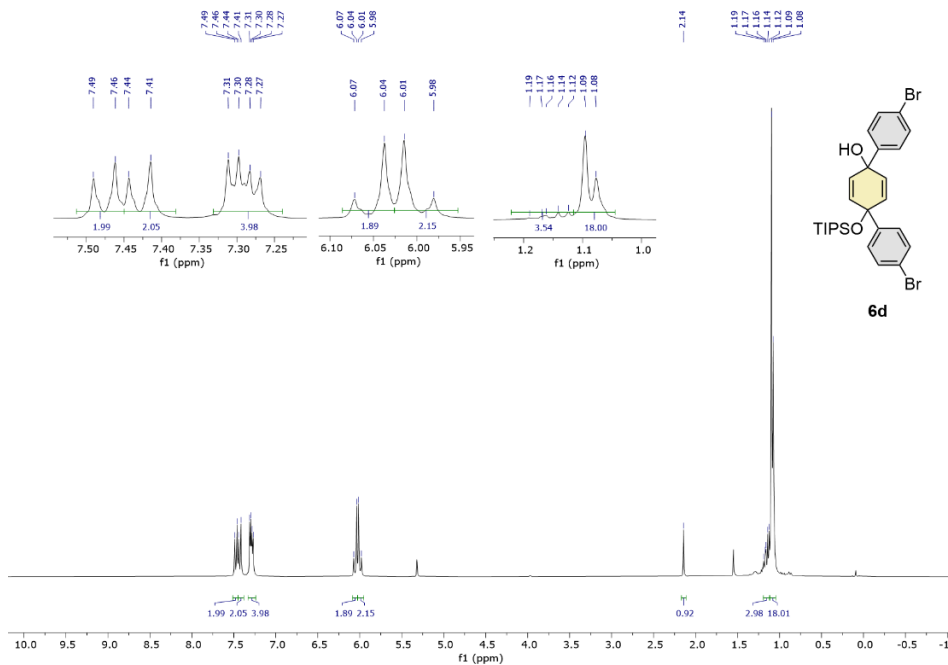


^1H NMR spectrum of compound **5d** in CDCl_3 (400 MHz).

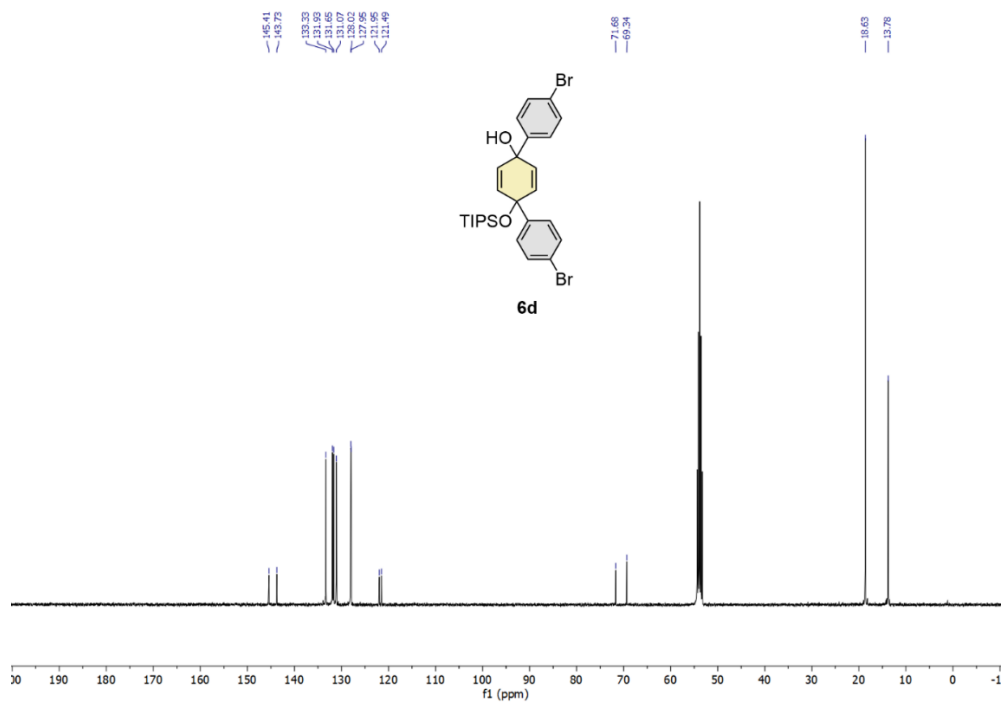
Chapter 2



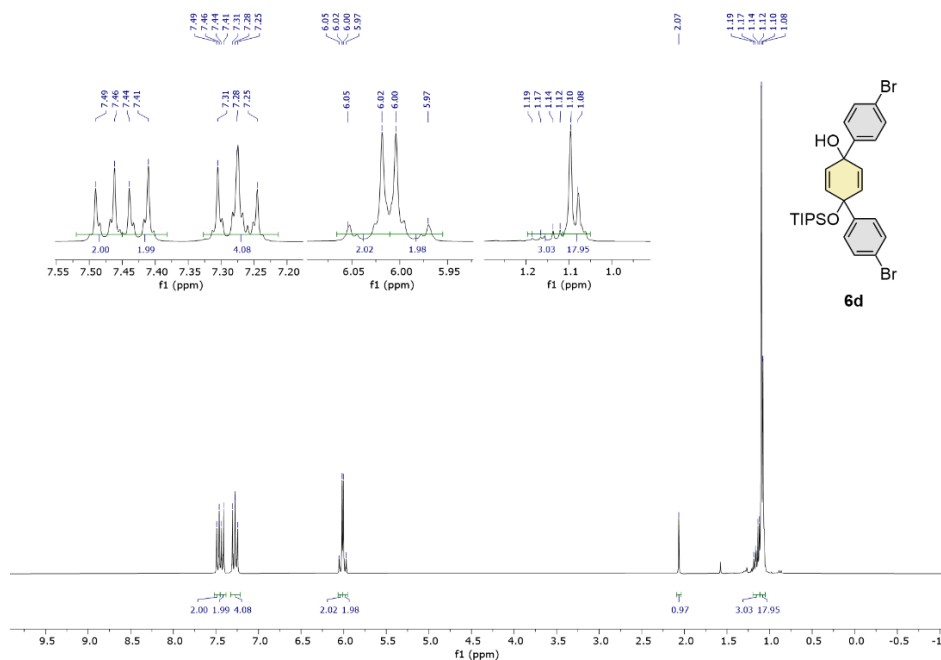
13C NMR spectrum of compound 5d in CDCl₃ (101 MHz).



1H NMR spectrum of compound 6d in CD₂Cl₂ (300 MHz).



¹³C NMR spectrum of compound **6d** in CD₂Cl₂ (101 MHz).



¹H NMR spectrum of compound **6d** in CDCl₃ (300 MHz).

2.5 References

- [1] T. J. Sisto, X. Tian, R. Jasti, *J. Org. Chem.* **2012**, *77*, 5857–5860.
- [2] J. Xia, M. R. Golder, M. E. Foster, B. M. Wong, R. Jasti, *J. Am. Chem. Soc.* **2012**, *134*, 19709–19715.
- [3] A. Yagi, Y. Segawa, K. Itami, *J. Am. Chem. Soc.* **2012**, *134*, 2962–2965.
- [4] H. Omachi, T. Nakayama, E. Takahashi, Y. Segawa, K. Itami, *Nat. Chem.* **2013**, *5*, 572–576.
- [5] M. R. Golder, C. E. Colwell, B. M. Wong, L. N. Zakharov, J. Zhen, R. Jasti, *J. Am. Chem. Soc.* **2016**, *138*, 6577–6582.
- [6] E. P. Jackson, T. J. Sisto, E. R. Darzi, R. Jasti, *Tetrahedron* **2016**, *72*, 3754–3758.
- [7] P. Li, B. M. Wong, L. N. Zakharov, R. Jasti, *Org. Lett.* **2016**, *18*, 1574–1577.
- [8] P. Li, L. N. Zakharov, R. Jasti, *Angew. Chem. Int. Ed.* **2017**, *56*, 5237–5241.
- [9] Y. Segawa, M. Kuwayama, Y. Hijikata, M. Fushimi, T. Nishihara, J. Pirillo, J. Shirasaki, N. Kubota, K. Itami, *Science* **2019**, *365*, 272–276.
- [10] Y. Yang, O. Blacque, S. Sato, M. Juriček, *Angew. Chem. Int. Ed.* **2021**, *60*, 13529–13535.
- [11] J. Malinčík, S. Gaikwad, J. P. Mora-Fuentes, M.-A. Boillat, A. Prescimone, D. Häussinger, A. G. Campaña, T. Šolomek, *Angew. Chem. Int. Ed.* **2022**, *61*, e202208591.
- [12] Y. Segawa, D. R. Levine, K. Itami, *Acc. Chem. Res.* **2019**, *52*, 2760–2767.
- [13] M. Fujitsuka, D. W. Cho, T. Iwamoto, S. Yamago, T. Majima, *Phys. Chem. Chem. Phys.* **2012**, *14*, 14585.
- [14] T. Nishihara, Y. Segawa, K. Itami, Y. Kanemitsu, *J. Phys. Chem. Lett.* **2012**, *3*, 3125–3128.
- [15] L. Adamska, I. Nayyar, H. Chen, A. K. Swan, N. Oldani, S. Fernandez-Alberti, M. R. Golder, R. Jasti, S. K. Doorn, S. Tretiak, *Nano Lett.* **2014**, *14*, 6539–6546.
- [16] V. S. Reddy, C. Camacho, J. Xia, R. Jasti, S. Irlle, *J. Chem. Theory Comput.* **2014**, *10*, 4025–4036.
- [17] M. R. Golder, R. Jasti, *Acc. Chem. Res.* **2015**, *48*, 557–566.
- [18] T. Iwamoto, Y. Watanabe, T. Sadahiro, T. Haino, S. Yamago, *Angew. Chem. Int. Ed.* **2011**, *50*, 8342–8344.
- [19] J. Xia, J. W. Bacon, R. Jasti, *Chem. Sci.* **2012**, *3*, 3018.
- [20] M. P. Alvarez, P. M. Burrezo, M. Kertesz, T. Iwamoto, S. Yamago, J. Xia, R. Jasti, J. T. L. Navarrete, M. Taravillo, V. G. Baonza, J. Casado, *Angew. Chem. Int. Ed.* **2014**, *53*, 7033–7037.
- [21] T. Iwamoto, Z. Slanina, N. Mizorogi, J. Guo, T. Akasaka, S. Nagase, H. Takaya, N. Yasuda, T. Kato, S. Yamago, *Chem. – Eur. J.* **2014**, *20*, 14403–14409.
- [22] H. Ueno, T. Nishihara, Y. Segawa, K. Itami, *Angew. Chem. Int. Ed.* **2015**, *54*, 3707–3711.
- [23] S. Hashimoto, T. Iwamoto, D. Kurachi, E. Kayahara, S. Yamago, *ChemPlusChem* **2017**, *82*, 1015–1020.
- [24] Y. Xu, S. Gsänger, M. B. Minameyer, I. Imaz, D. Maspoch, O. Shyshov, F. Schwer, X. Ribas, T. Drewello, B. Meyer, M. von Delius, *J. Am. Chem. Soc.* **2019**, *141*, 18500–18507.
- [25] M. B. Minameyer, Y. Xu, S. Frühwald, A. Görling, M. von Delius, T. Drewello, *Chem. – Eur. J.* **2020**, *26*, 8729–8741.
- [26] E. Ubasart, O. Borodin, C. Fuertes-Espinosa, Y. Xu, C. García-Simón, L. Gómez, J. Juanhuix, F. Gándara, I. Imaz, D. Maspoch, M. von Delius, X. Ribas, *Nat. Chem.* **2021**, *13*, 420–427.
- [27] Y. Xu, M. von Delius, *Angew. Chem. Int. Ed.* **2020**, *59*, 559–573.

- [28] E. J. Leonhardt, J. M. Van Raden, D. Miller, L. N. Zakharov, B. Alemán, R. Jasti, *Nano Lett.* **2018**, *18*, 7991–7997.
- [29] B. M. White, Y. Zhao, T. E. Kawashima, B. P. Branchaud, M. D. Pluth, R. Jasti, *ACS Cent. Sci.* **2018**, *4*, 1173–1178.
- [30] J. M. Van Raden, B. M. White, L. N. Zakharov, R. Jasti, *Angew. Chem. Int. Ed.* **2019**, *58*, 7341–7345.
- [31] T. C. Lovell, Z. R. Garrison, R. Jasti, *Angew. Chem. Int. Ed.* **2020**, *59*, 14363–14367.
- [32] J. M. V. Raden, N. N. Jarenwattananon, L. N. Zakharov, R. Jasti, *Chem. – Eur. J.* **2020**, *26*, 10205–10209.
- [33] T. A. Schaub, E. A. Prantl, J. Kohn, M. Bursch, C. R. Marshall, E. J. Leonhardt, T. C. Lovell, L. N. Zakharov, C. K. Brozek, S. R. Waldvogel, S. Grimme, R. Jasti, *J. Am. Chem. Soc.* **2020**, *142*, 8763–8775.
- [34] J. M. Van Raden, E. J. Leonhardt, L. N. Zakharov, A. Pérez-Guardiola, A. J. Pérez-Jiménez, C. R. Marshall, C. K. Brozek, J. C. Sancho-García, R. Jasti, *J. Org. Chem.* **2020**, *85*, 129–141.
- [35] R. L. Maust, P. Li, B. Shao, S. M. Zeitler, P. B. Sun, H. W. Reid, L. N. Zakharov, M. R. Golder, R. Jasti, *ACS Cent. Sci.* **2021**, *7*, 1056–1065.
- [36] C. E. Otteson, C. M. Levinn, J. M. Van Raden, M. D. Pluth, R. Jasti, *Org. Lett.* **2021**, *23*, 4608–4612.
- [37] E. J. Leonhardt, R. Jasti, *Nat. Rev. Chem.* **2019**, *3*, 672–686.
- [38] R. Jasti, J. Bhattacharjee, J. B. Neaton, C. R. Bertozzi, *J. Am. Chem. Soc.* **2008**, *130*, 17646–17647.
- [39] T. J. Sisto, M. R. Golder, E. S. Hirst, R. Jasti, *J. Am. Chem. Soc.* **2011**, *133*, 15800–15802.
- [40] P. Wipf, J.-K. Jung, *Chem. Rev.* **1999**, *99*, 1469–1480.
- [41] M. R. Golder, L. N. Zakharov, R. Jasti, *Pure Appl. Chem.* **2017**, *89*, 1603–1617.
- [42] E. Kayahara, V. K. Patel, S. Yamago, *J. Am. Chem. Soc.* **2014**, *136*, 2284–2287.
- [43] V. K. Patel, E. Kayahara, S. Yamago, *Chem. – Eur. J.* **2015**, *21*, 5742–5749.
- [44] T. Sisto, R. Jasti, *Synlett* **2012**, *23*, 483–489.
- [45] D. Kohrs, J. Becker, H. A. Wegner, *Chem. – Eur. J.* **2022**, *28*, e202104239.
- [46] M. Lalonde, T. H. Chan, *Synthesis* **2002**, *1985*, 817–845.
- [47] T. D. Nelson, R. D. Crouch, *Synthesis* **2000**, *1996*, 1031–1069.
- [48] R. David Crouch, *Tetrahedron* **2004**, *60*, 5833–5871.
- [49] R. D. Crouch, *Synth. Commun.* **2013**, *43*, 2265–2279.
- [50] J. S. Davies, C. L. Higginbotham, E. John Tremeer, C. Brown, R. C. Treadgold, *J. Chem. Soc. Perkin 1* **1992**, *0*, 3043–3048.
- [51] P. G. M. Wuts, T. W. Greene, John Wiley & Sons, **2006**.
- [52] E. J. Corey, H. Cho, C. Rücker, D. H. Hua, *Tetrahedron Lett.* **1981**, *22*, 3455–3458.
- [53] E. R. Darzi, T. J. Sisto, R. Jasti, *J. Org. Chem.* **2012**, *77*, 6624–6628.
- [54] J. Xia, R. Jasti, *Angew. Chem. Int. Ed.* **2012**, *51*, 2474–2476.
- [55] P. J. Evans, E. R. Darzi, R. Jasti, *Nat. Chem.* **2014**, *6*, 404–408.
- [56] P. Li, T. J. Sisto, E. R. Darzi, R. Jasti, *Org. Lett.* **2014**, *16*, 182–185.
- [57] E. R. Darzi, E. S. Hirst, C. D. Weber, L. N. Zakharov, M. C. Lonergan, R. Jasti, *ACS Cent. Sci.* **2015**, *1*, 335–342.
- [58] D. A. Hines, E. R. Darzi, E. S. Hirst, R. Jasti, P. V. Kamat, *J. Phys. Chem. A* **2015**, *119*, 8083–8089.
- [59] J. M. Van Raden, E. R. Darzi, L. N. Zakharov, R. Jasti, *Org. Biomol. Chem.* **2016**, *14*, 5721–5727.

- [60] E. Kayahara, L. Sun, H. Onishi, K. Suzuki, T. Fukushima, A. Sawada, H. Kaji, S. Yamago, *J. Am. Chem. Soc.* **2017**, *139*, 18480–18483.
- [61] T. A. Schaub, J. T. Margraf, L. Zakharov, K. Reuter, R. Jasti, *Angew. Chem. Int. Ed.* **2018**, *57*, 16348–16353.
- [62] S. Hashimoto, E. Kayahara, Y. Mizuhata, N. Tokitoh, K. Takeuchi, F. Ozawa, S. Yamago, *Org. Lett.* **2018**, *20*, 5973–5976.
- [63] T. C. Lovell, C. E. Colwell, L. N. Zakharov, R. Jasti, *Chem. Sci.* **2019**, *10*, 3786–3790.
- [64] R. Jasti, C. R. Bertozzi, *Chem. Phys. Lett.* **2010**, *494*, 1–7.
- [65] E. S. Hirst, R. Jasti, *J. Org. Chem.* **2012**, *77*, 10473–10478.
- [66] Y. Segawa, A. Yagi, K. Matsui, K. Itami, *Angew. Chem. Int. Ed.* **2016**, *55*, 5136–5158.
- [67] E. J. Corey, A. Venkateswarlu, *J. Am. Chem. Soc.* **1972**, *94*, 6190–6191.
- [68] Y. Abe, *Bull. Chem. Soc. Jpn.* **1943**, *18*, 93–97.
- [69] S. Goodwin, B. Witkop, *J. Am. Chem. Soc.* **1957**, *79*, 179–185.
- [70] B. Miller, *Acc. Chem. Res.* **1975**, *8*, 245–256.
- [71] A. Planas, J. Tomás, J.-J. Bonet, *Tetrahedron Lett.* **1987**, *28*, 471–474.
- [72] I. Kim, K. Kim, J. Choi, *J. Org. Chem.* **2009**, *74*, 8492–8495.
- [73] W. M. Haynes, Ed., CRC Press, Boca Raton, **2016**.
- [74] A. Trummal, L. Lipping, I. Kaljurand, I. A. Koppel, I. Leito, *J. Phys. Chem. A* **2016**, *120*, 3663–3669.
- [75] R. B. Kręćijasz, T. Šolomek; unpublished work.
- [76] E. R. Darzi, B. M. White, L. K. Loventhal, L. N. Zakharov, R. Jasti, *J. Am. Chem. Soc.* **2017**, *139*, 3106–3114.
- [77] A. Abdulkarim, F. Hinkel, D. Jänsch, J. Freudenberg, F. E. Golling, K. Müllen, *J. Am. Chem. Soc.* **2016**, *138*, 16208–16211.